



HAL
open science

Tomotectonics of Cordilleran North America since Jurassic times: double-sided subduction, archipelago collisions, and Baja-BC translation

Karin Sigloch, Mitchell Mihalynuk

► To cite this version:

Karin Sigloch, Mitchell Mihalynuk. Tomotectonics of Cordilleran North America since Jurassic times: double-sided subduction, archipelago collisions, and Baja-BC translation. 2024. hal-04662502

HAL Id: hal-04662502

<https://hal.science/hal-04662502>

Preprint submitted on 25 Jul 2024

HAL is a multi-disciplinary open access archive for the deposit and dissemination of scientific research documents, whether they are published or not. The documents may come from teaching and research institutions in France or abroad, or from public or private research centers.

L'archive ouverte pluridisciplinaire **HAL**, est destinée au dépôt et à la diffusion de documents scientifiques de niveau recherche, publiés ou non, émanant des établissements d'enseignement et de recherche français ou étrangers, des laboratoires publics ou privés.



Distributed under a Creative Commons Attribution - NonCommercial - NoDerivatives 4.0 International License

PREPRINT: This manuscript has been submitted to GSA Books volume “Jurassic–Paleogene tectonic evolution of the North American Cordillera” and has not yet been peer reviewed by the Geological Society of America.

Tomotectonics of Cordilleran North America since Jurassic times: double-sided subduction, archipelago collisions, and Baja-BC translation

Karin Sigloch¹ & Mitchell G. Mihalynuk²

1) Université Côte d’Azur, CNRS, Observatoire Côte d’Azur, IRD. Géoazur, Sophia Antipolis, France

2) British Columbia Geological Survey. Ministry of Energy, Mines and Low Carbon Innovation British Columbia. Victoria, Canada

Abstract

Tomotectonics uses deep mantle structure in order to hindcast paleo-trenches, by spatially superposing subducted lithosphere (slabs) imaged by seismic tomography with plate reconstructions at the surface. The two geophysical datasets combined make predictions about geologic events, specifically about volcanic arcs and their collisions with continents. The tomotectonic null hypothesis is simple, predictive and testable. It uses land geological observations for validation. We explain the method, with a clear conceptual separation of its hypothesis-generating stage (using geophysics and the hypothesis of vertical slab sinking) from its subsequent hypothesis-testing stage (using geological observations from accretionary orogens).

With the North American Cordillera as a case study, we generate a full suite of tomotectonic inferences on the slab assemblage that now occupies the mantle under North America to depths of 1800-2000 km. We reason why this assemblage originated as a completely intra-oceanic archipelago of paleo-trenches at a time of worldwide tectonic reorganization: around 200-170 Ma, when the Atlantic began to spread and the Pacific plate was born. An Archipelago is circumscribed by trenches that pull in seafloor from (at least) two sides: here, roughly from the east and from the west. North America was pulled westward by, and overrode, the westward-subducting arcs. These collisions since ~150 Ma caused the Nevadan and Sevier orogenies, and spawned the eastward-subducting arc that built Sierra Nevada Batholith ~120-80 Ma.

From ~110-50 Ma, the continent collided with the arc of future Central Alaska and with the Farallon arc of the Pacific Northwest, which sat offshore until ~90-50 Ma. Override of this double-sided arc pair enabled a range of collision styles, including the Baja-BC northward sprint and its accretion to Central Alaska. Tomotectonics infers large-scale northward displacement of Insular Superterrane since its accretion, which provides independent support for the “Baja-BC” hypothesis of paleomagnetism.

Figure 1

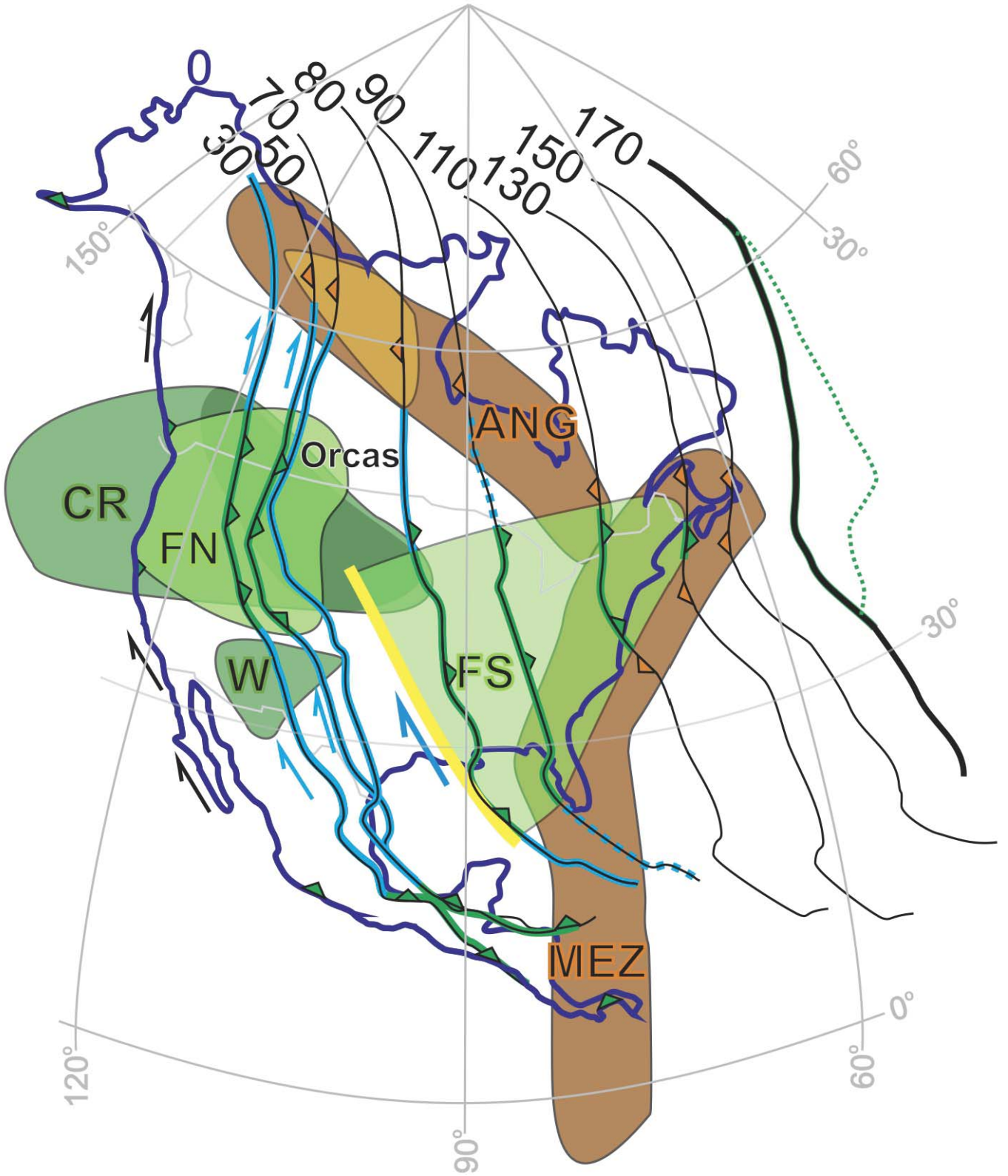


Figure 2

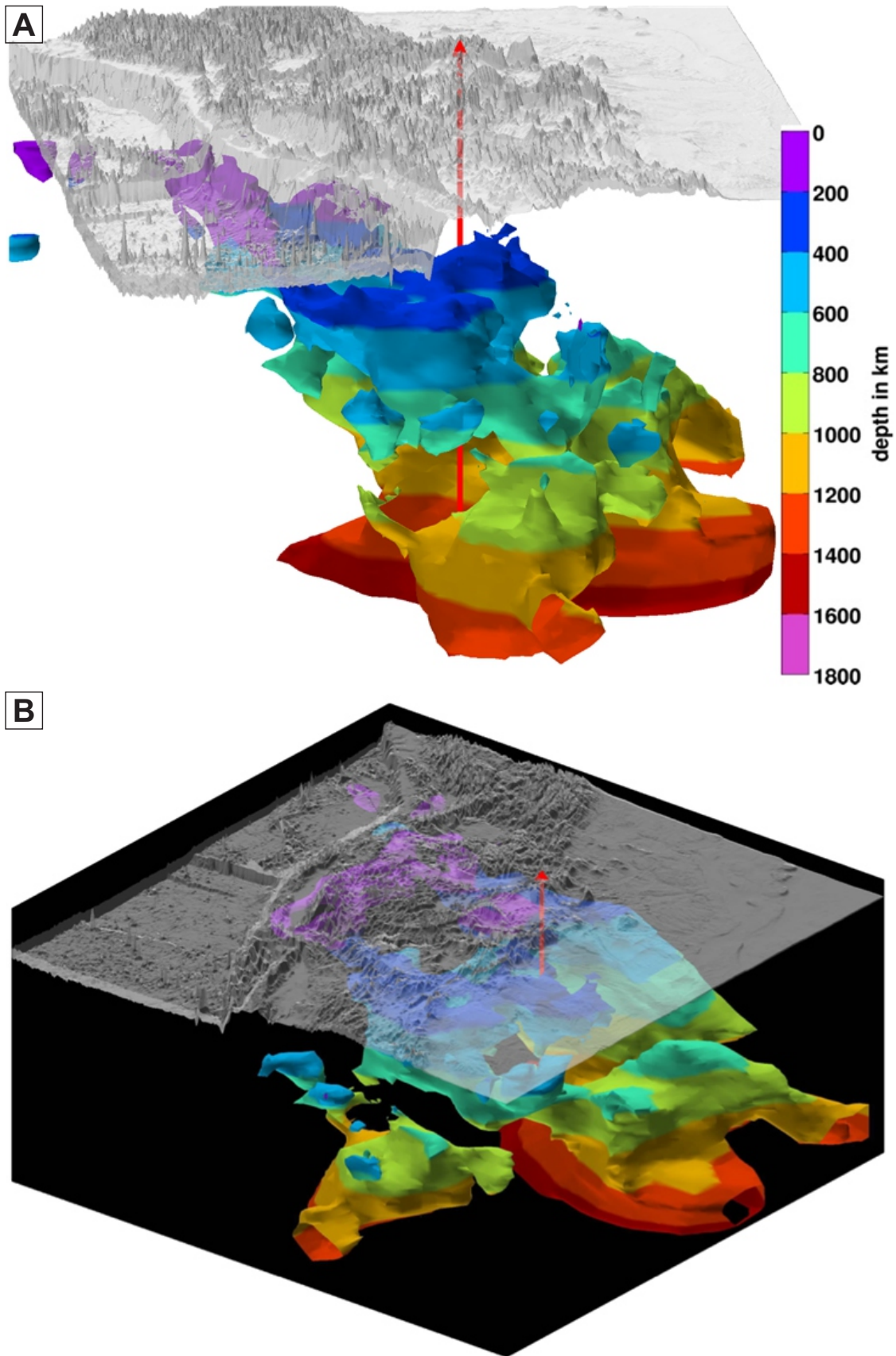


Figure 3

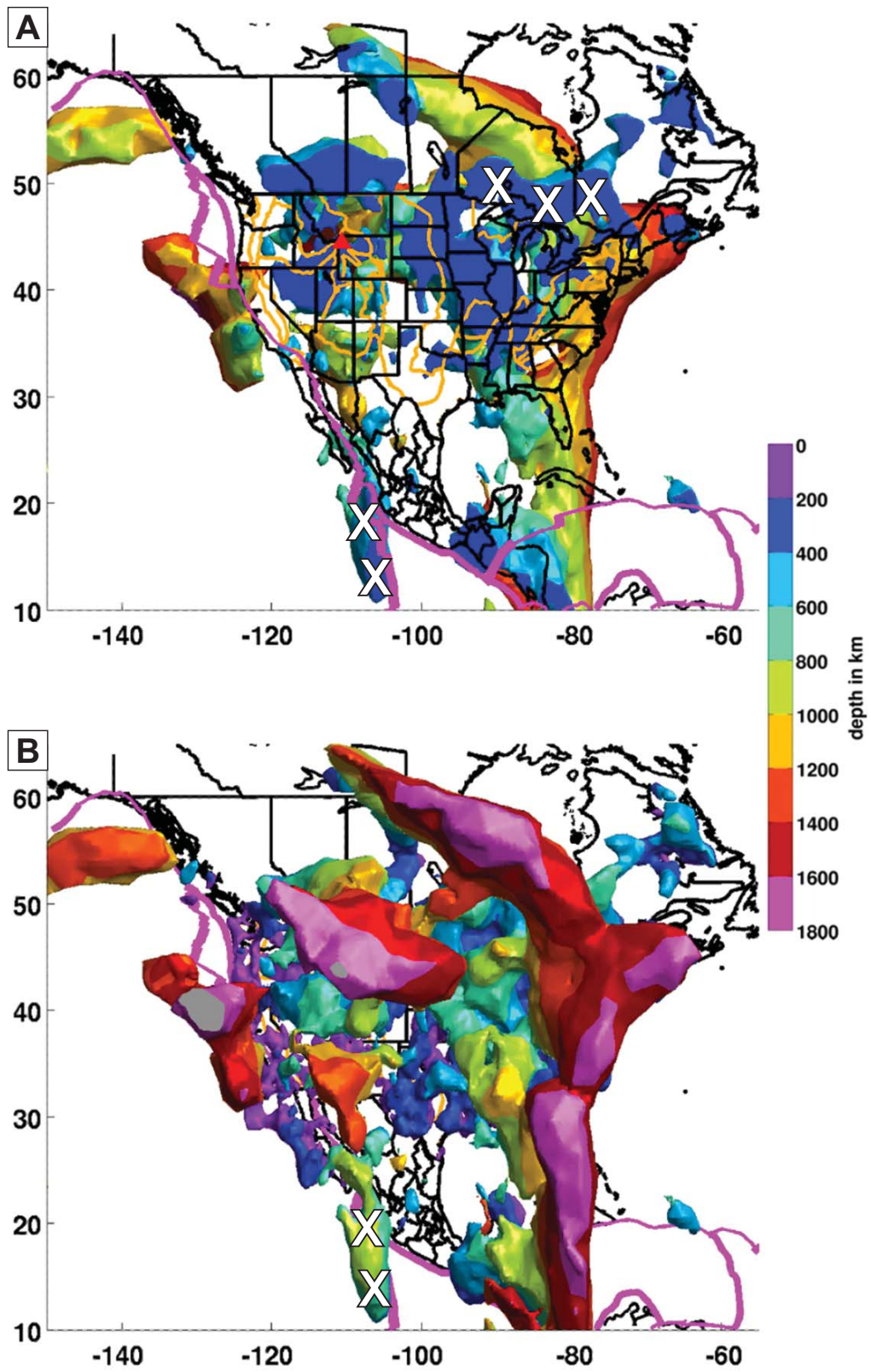


Figure 4

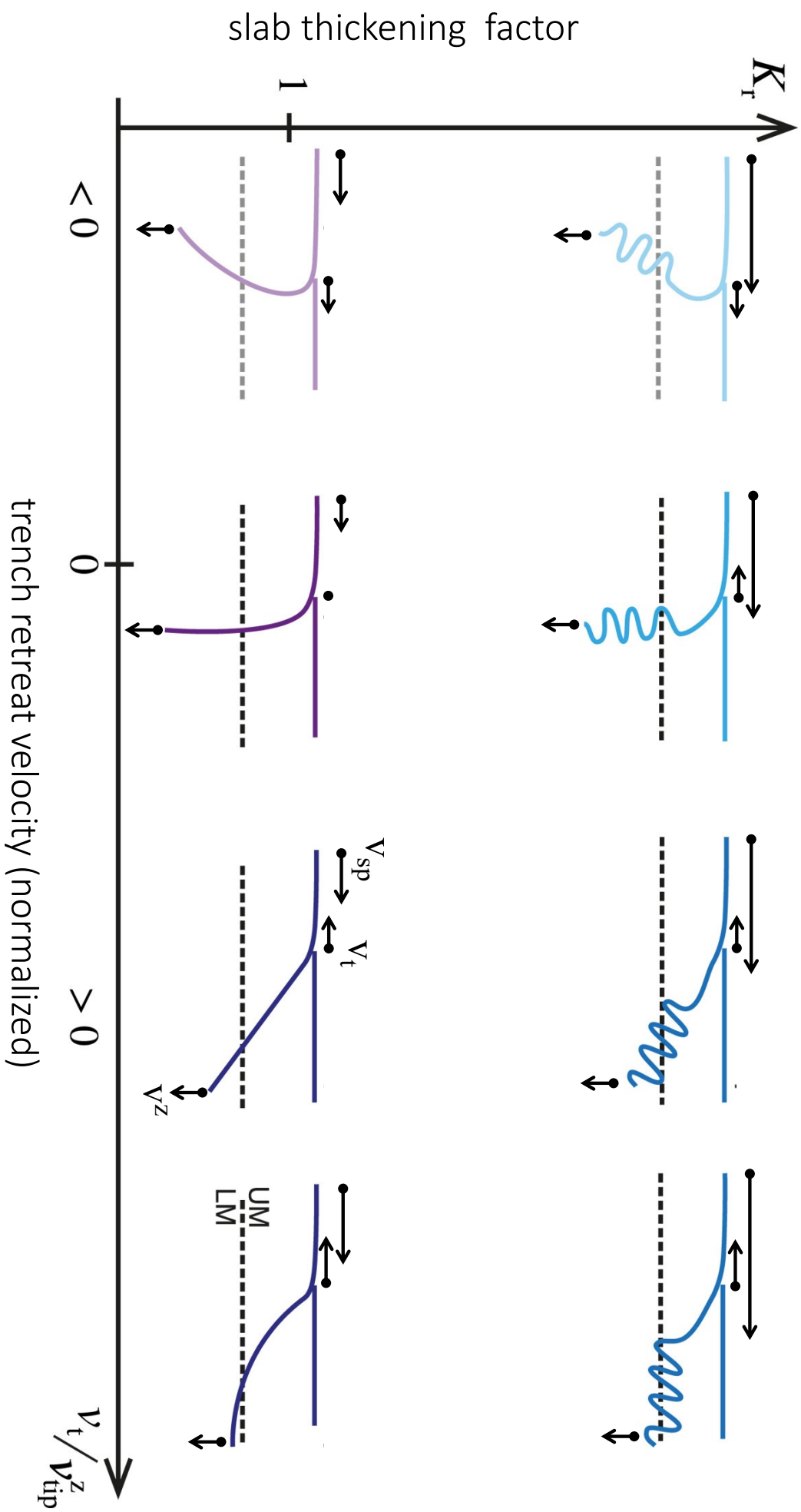


Figure 5

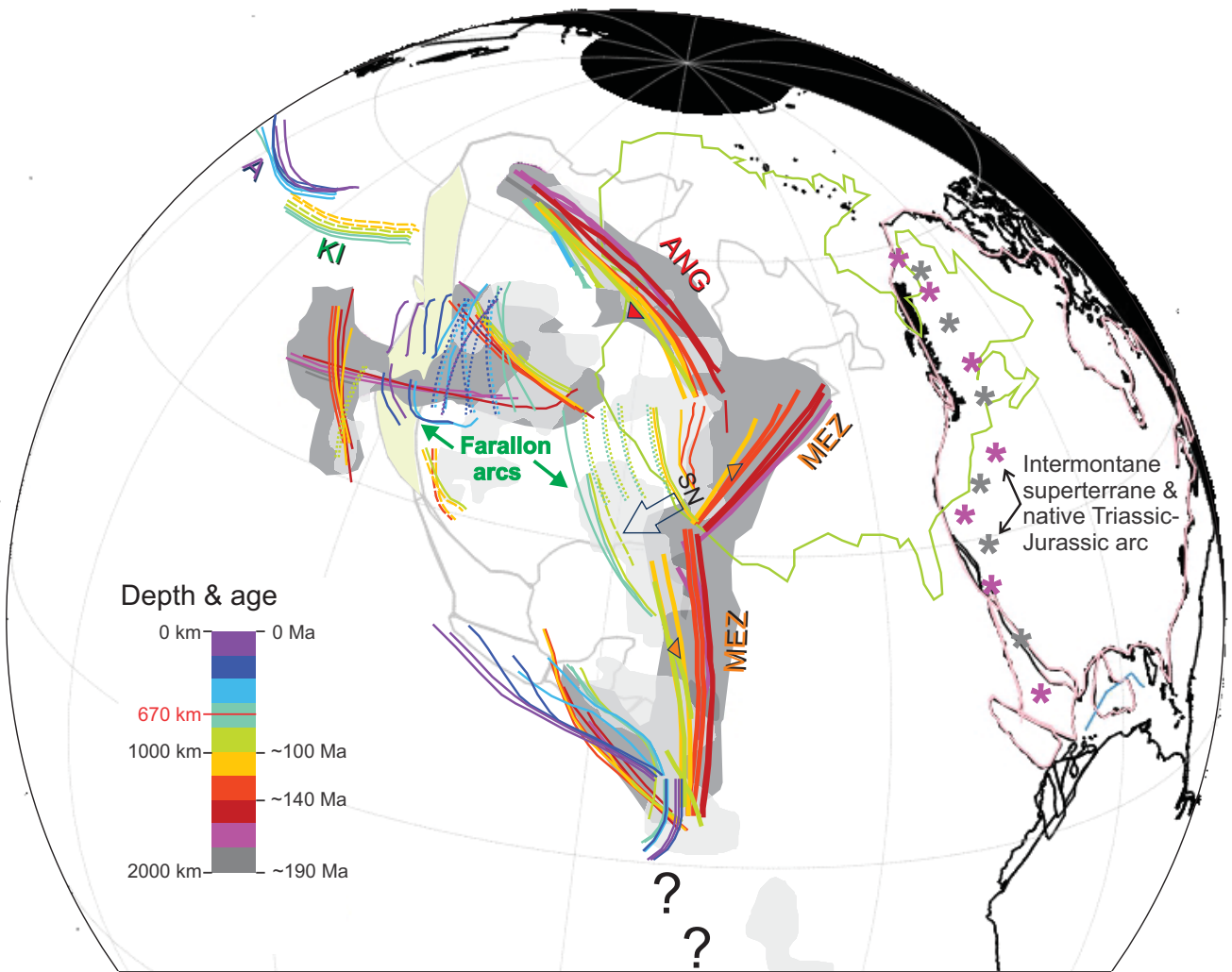
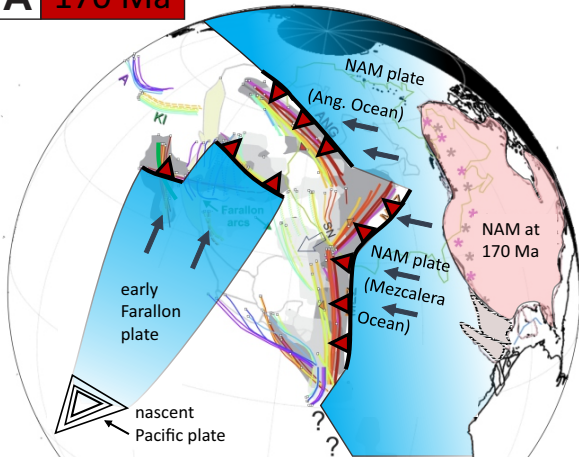


Figure 6

A 170 Ma



B 80 Ma

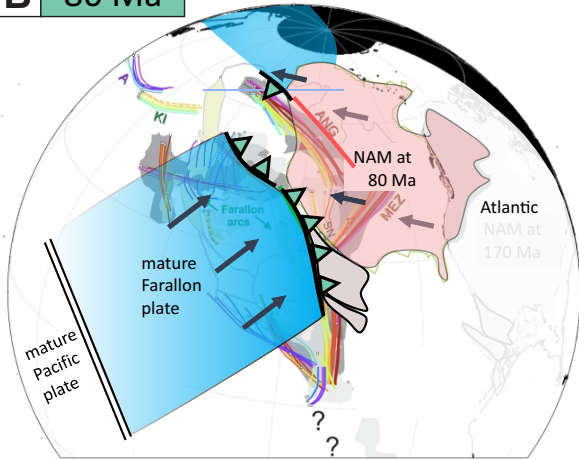


Figure 7

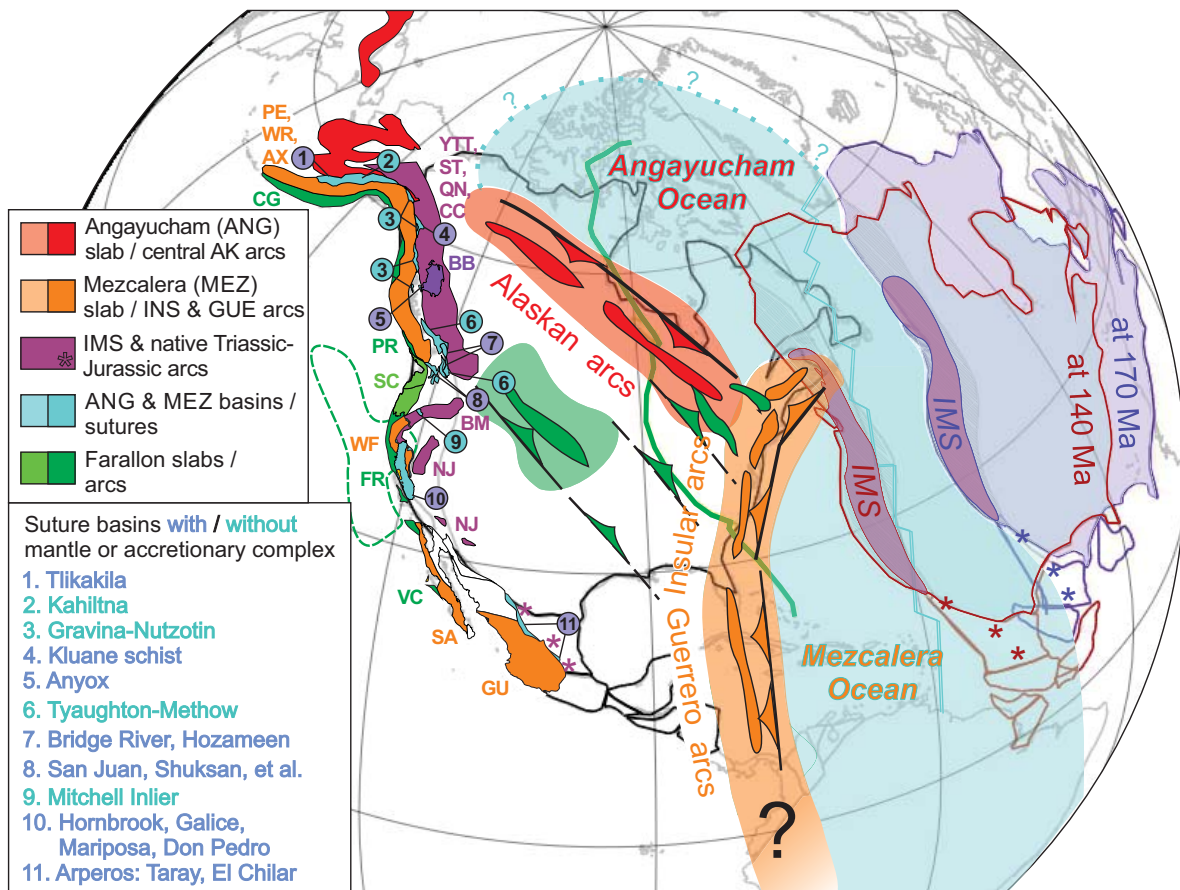


Figure 8

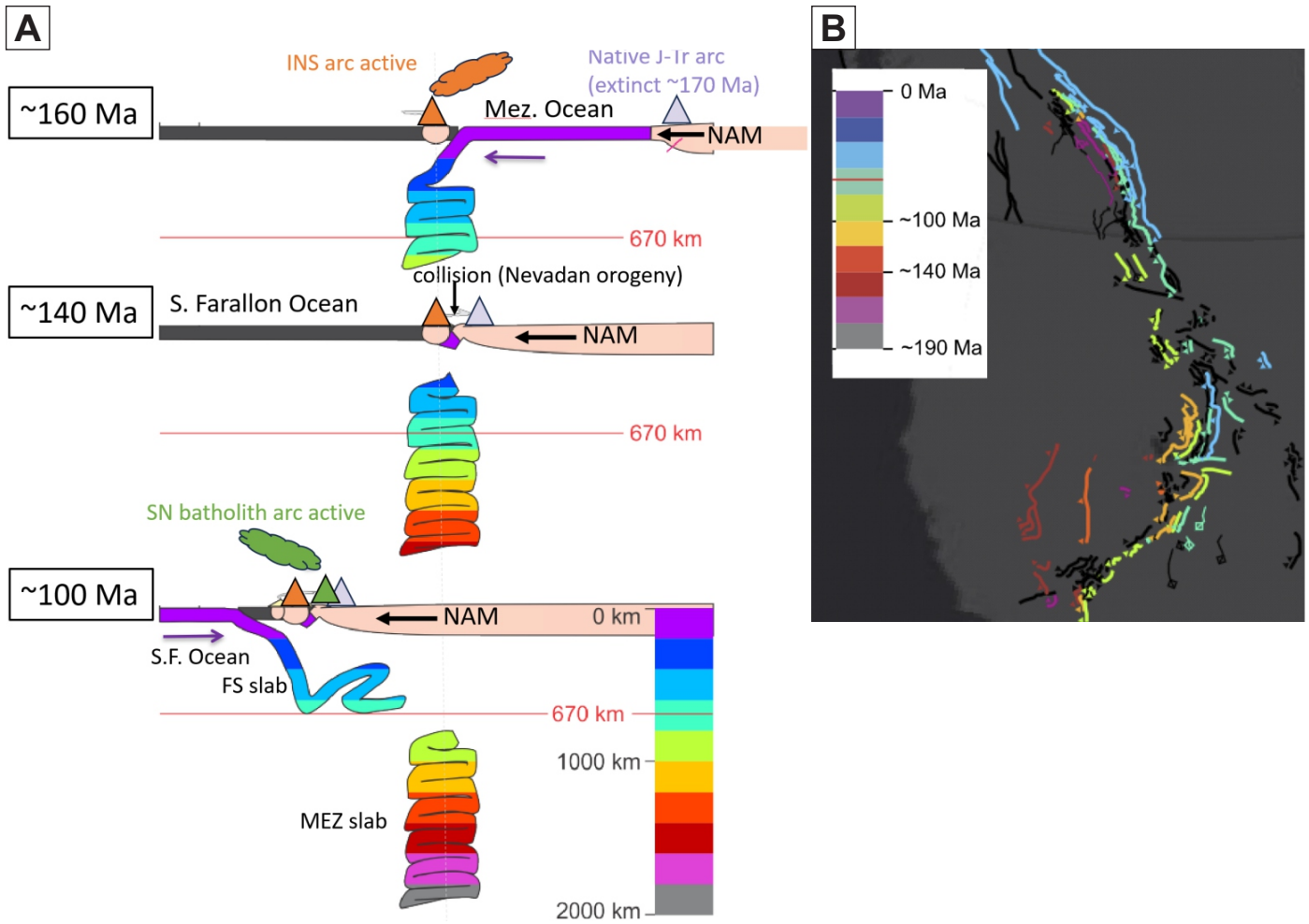


Figure 9

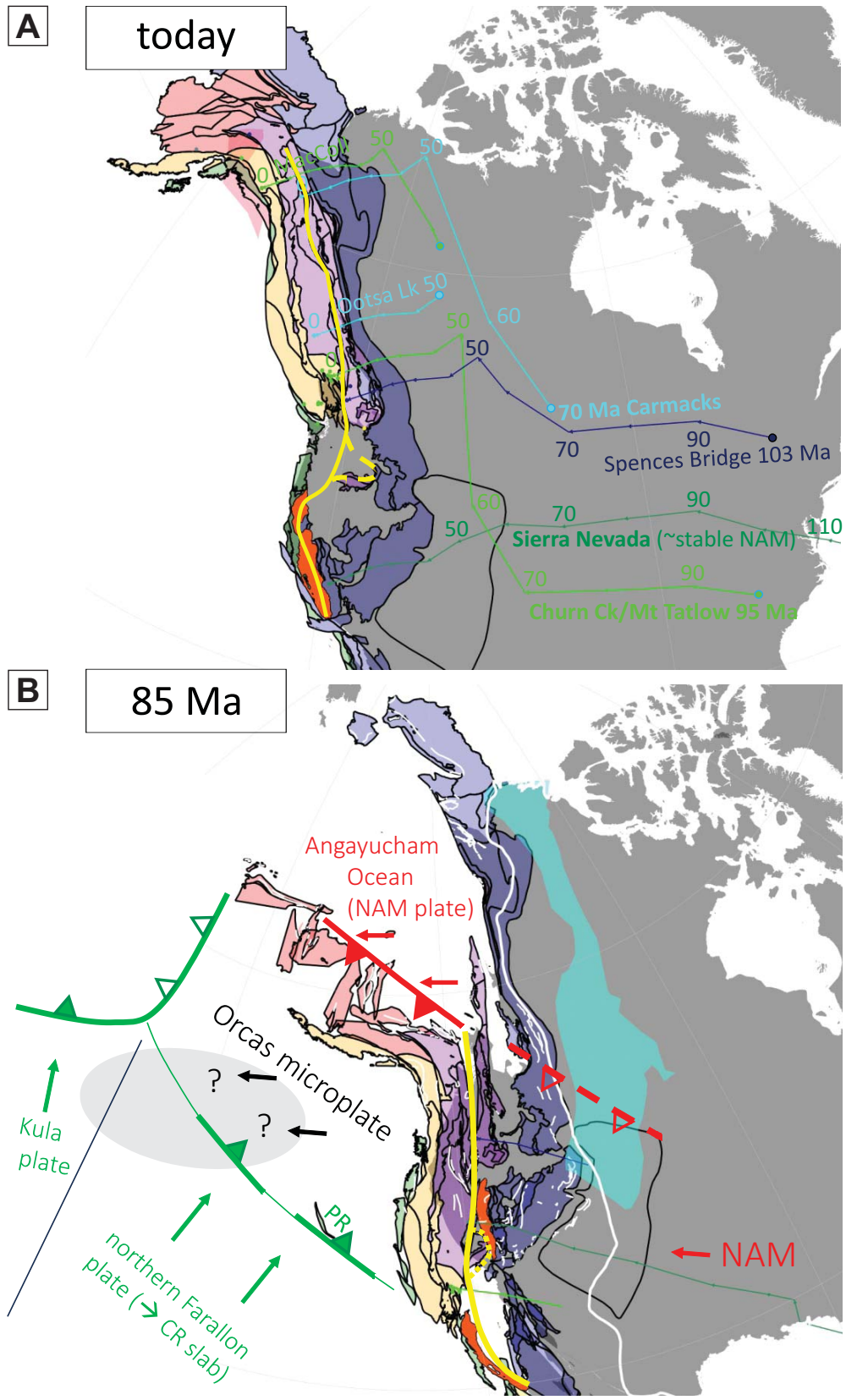


Figure captions

Figure 1. Observations for tomotectonics: subducted lithosphere (slabs) in the mantle and a quantitative plate reconstruction at the surface. Coloured polygons show outlines of major slabs under North America from the regional tomographic P-wave model of Sigloch (2011). Orange slabs were deposited by westward subduction, green slabs by eastward (Farallon) subduction. Dark shades are applied to lower-mantle slabs MEZ, ANG and CR/W; light shades to (mostly) shallower slabs FS (400-1000 km deep), FN (0-700 km), and to the shallow western end of ANG (>400 km deep).

Superimposed are snapshots in time showing the westward migrating margin of North America in a mantle reference frame constrained between 0-120 Ma by moving hotspots (Dubrovine et al., 2012) and 120-170 Ma by true polar wander-corrected paleomagnetic data (Torsvik et al., 2019). Under the tomotectonic null hypothesis, a continental margin above a slab indicates a continent-trench interaction. In such cases, barbs are drawn on the continental margin in order to signal the nature of the interaction: NAM-beneath-arc collision (orange barbs, associated with westward subduction) or ocean plate beneath margin, with arc built on NAM (green barbs, associated with eastward subduction). A transform regime along the ocean-continent boundary is marked in light blue, with blue arrows for displacement direction. Transform motion can be inferred from the continent margin overlying a slab-free zone, but only if the margin is known to be a plate boundary (prior to ~150 Ma, it was not). Yellow line signals the western edge of FS slab, associated with the “Big Break” event of transition from subduction to transform ~80 Ma. During a short time window around ~70 Ma, the entire margin is inferred to have been in a transform regime. The starting point of our inference is ~170 Ma, the time when North America separated from Pangaea, and when absolute paleo-positioning in plate reconstructions becomes reasonably accurate.

Figure 2. Subducted oceanic lithosphere (slab) deposited in the mantle by past and present Farallon subduction at latitudes of the Pacific Northwest, from the surface to ~1800 km depth. Seismically fast structure (subducted oceanic lithosphere) is rendered as 3-D isosurfaces (threshold $dV_p/V_p > 0.25\%$) on the teleseismic P-wave model of Sigloch 2011. Color signals depth and changes in increments of 200 km. Surface topography of the North American Cordillera and the Pacific basin are overlain in translucent gray, with strong vertical exaggeration. Yellowstone (red triangle) and its vertical downward continuation are shown for visual reference. Not rendered are seismically slow anomalies (such as the Yellowstone mantle plume, which is wedged inside the “cavities” of the slabscape).

The slab has an overall eastward dip. In detail, its geometries are complex and fragmented, but highly structured. The slab is clearly delineated against adjacent and deeper slab-free areas. It enters the mantle with the thickness of lithosphere (<100 km, purple parts), but thickens in the transition zone (blues) and is most massive in the lower mantle (green, yellow, red). The shallow fast anomalies of the Wyoming craton and lithosphere of stable NAM had to be masked out as they are located between the viewpoint of the figure and the slabscape.

Figure 3. Mantle tomography: 3-D isosurface rendering of all seismically fast P-wave anomalies in the upper and lower mantle beneath North America to ~1800 km depth. The rendering threshold is $dV_p/V_p = +0.25\%$. Below lithospheric depths, fast anomalies can generally be taken to mean slab (subducted lithosphere). (A) top-down view of all fast structure below 400 km (in order to exclude the overlying lithosphere, which is fast but not slab). Color signals depth and changes every 200 km. (B) inside-out

view of all fast structure from the surface down, with the deepest structure (slab walls) emerging to the foreground. Imaging limitations include artifacts, especially near the margins of the regional dataset: resolution lost into the ocean basins and north of 55°. Two downward smearing artifacts are labeled with white x's and should not be interpreted. (After Sigloch, 2011.)

Figure 4. Illustration of the tomotectonic null hypothesis. Range of possible shapes for slabs that sink *vertically* after entering the trench (and grow long enough to enter the lower mantle). Dashed line represents the viscosity discontinuity between upper mantle (UM) and lower mantle (LM), where the mantle becomes 1-2 orders of magnitude more viscous, resisting further slab sinking. This cartoon explores the parameter space of relevant ratios of the three velocities that determine slab geometry: (1) convergence velocity onto the trench of the subducting plate (v_{sp}); (2) trench retreat velocity of the overriding plate (v_t); (3) velocity at which the slab tip in the LM can sink vertically $v^{z_{tip}}$. Vectorial arrows for v_t , v_{sp} , $v^{z_{tip}}$ are shown qualitatively for each slab cartoon; $v^{z_{tip}}$ is arbitrarily chosen as constant across the different cases.

Trench retreat velocity v_t (normalized by $v^{z_{tip}}$) is shown on the x-axis. If the trench is stationary ($v_t = 0$), a vertical slab piles up beneath it. Trench retreat ($v_t > 0$) produces a trenchward dipping slab: the dip results from recently subducted slab not yet having sunk as far as older slab. Trench advance ($v_t < 0$, rarely observed) produces an overturned dipping slab. Kinematic ratio K_r on the y-axis expresses whether v_{sp} , the length of slab newly entering the mantle per time unit, can be accommodated in the slab-free space created by trench migration v_t (horizontally away from already-deposited slab) and/or by the vertical sinking away of older slab ($v^{z_{tip}}$), which vacates upper-mantle space. $K_r > 1$ indicates “traffic jam conditions”, where plate convergence is too rapid to be accommodated undeformed, so the slab is forced to thicken (probably by folding). Tomography observes thickened slabs to be ubiquitous in the lower mantle. Consistent with this, Cerpa et al. (2022) found that $K_r > 1$ for almost all present-day trenches. See Cerpa et al. (2022) for exact definition of K_r .

Figure 5. Paleo-trenches in absolute (mantle) coordinates, as predicted by tomotectonics and its vertical slab sinking hypothesis. This represents a quasi-literal transcription of the 3-D slabscape with depth. Tracks of paleo-arc locations are shown as thick lines if produced by westward subduction, and thin lines if produced by eastward subduction or subduction of ambiguous polarity (mostly Farallon). For laterally extended slabs, those produced when the arc translates rapidly with respect to the mantle reference frame, a distinct locus of slab deposition is not clearly resolvable, and the arc lines are shown as dashed. Depth-to-colour mapping as for the slab-scapes of figures 2 & 3. The colour bar also shows an indicative depth-to-time mapping. This time conversion is empirically justified by the observation that slabs seem to have sunk rather uniformly at a rate of ~ 10 mm/yr. This averaged sinking rate is a parameter estimated from slab geometries and plate motions; a constant sinking rate is *not* assumed, neither is it part of the tomotectonic hypothesis. It is not strictly needed for this study, but remains useful as a rough and robust link to geologic time. The continent is reconstructed at three times 170 Ma, ~ 80 Ma (green outline), and present day. Grey tones denote 2D extents of slabs of concern at 800 km depth (light grey) and 1400 km (medium grey). Arc / slab labels: A = Aleutian, ANG = Angayucham, KI = Kula-Izanagi, MEZ = Mezcalera. SN = approximate position of the Sierra Nevada batholith; the arrow denotes possible extents of the Hess-Shatsky Rise conjugate plateau.

Figure 6. Constraints on the growth and consumption of ocean basins subducting into the Archipelago, shown in two cartoon time frames for 170 Ma (early Archipelago before NAM started moving west) and for 80 Ma (override far advanced, westward subduction almost overridden). Trenches highlighted with

barbs and colours were active at 170 Ma (red) or 80 Ma (green); they are plotted on the basemap of fig. 4. The lateral distance from continent (or Farallon spreading ridge) to its nearest slab defines the extents of two paleo-oceans: the Farallon Ocean subducted eastward, the Mezcalera-Angayucham Ocean (NAM plate) westward. Lateral overlap of continent and trench predicts a continent-arc collision. Trenches at 170 Ma run above the three slab walls that all reach to ~1800-2000 km depth – representing the early, purely intra-oceanic stage of the archipelago. Farallon and ANG subduction face each other off in double-sided subduction from the start. The width of CR slab corresponds to the (narrow) width of early Farallon isochrons (FAR-PAC-Izanagi spreading “triangle” at 170 Ma). Baja-BC shuffling and assembly of Alaska will play in the small space between these two arcs, on the Orcas microplate. The mature Pacific-Farallon spreading ridge at 80 Ma “serves” both CR and FS, where FS is a margin-hugging trench, whereas CR (the original, northern Farallon) still remains offshore.

Figure 7. Arc terranes matched to slabs. Arc (super-)terrane are shown in their present positions in the Cordillera on the left part of the map. The same arc terranes are schematically reconstructed above their matched slabs and paleo-trenches, in absolute positions relative to the lower mantle. The reconstruction time for the arcs and slab walls corresponds to ~170 Ma (before Archipelago override began), except in the case of the SW-ward migrating southern Farallon (SNB) arc, which is shown in several time snapshots migrating across the area it covered over its lifetime (~130-80 Ma). Current and former instances of arcs are linked by their unchanging colors over time: Farallon arcs and slabs in green, Insular (INS) & Guerrero (GUE) microcontinents and slabs in orange; Intermontane (IMS) microcontinent in purple; and Central Alaskan arcs and slabs in red. Westward drift of North America is shown at 170 Ma, 140 Ma and 80 Ma (green coastline), as calibrated from Atlantic ocean isochrons and a mantle reference frame. Every substantive slab should be associated with a geologically known arc, and every known arc should be associated with a slab. The above slab/terrane associations appear to satisfy geologic constraints, and to yield the Cordillera’s present-day terrane assemblage when the 150 million years of slab-predicted collision sequences are played forward.

Abbreviations: Guerrero-Insular arc terranes (orange) include basement substrate, with arcs constructed atop by westward subduction: AX (Alexander), GU (Guerrero), PE (Peninsular), WF (Western Jurassic, Western Hayfork, Foothills, and related terranes), WR (Wrangellia), SA (Santa Ana). IMS Superterrane (purple) include terranes docked at the margin of North America before or immediately following the start of Atlantic spreading: BM (Blue Mountains), CC (Cache Creek), QN (Quesnel), ST (Stikine) and YTT (Yukon Tanana). Terranes linked to the Native Jurassic arc (NJ) and its along-strike continuation of extensional magmatism in Mexico (“Nazas arc”) are diagrammatically shown by purple asterisks. Green terranes are associated with Farallon subduction (eastward): CG—Chugach; FR—Franciscan; PR—Pacific Rim; SC—Siletz-Crescent; VC—Vizcaino. Cyan polygons are suture basins – the relics of large paleo-ocean basins shown in translucent cyan; they straddle the boundary between orange (MEZ) and purple (IMS/NJ) terranes as predicted. Where adjacent IMS was below sea level, the suture basin strata may have extended as the Bowser Basin (BB). Sierra Nevada batholith, located immediately east of basin 10, overprints the basin and the Native Jurassic arc. (Modified from Sigloch & Mihalynuk, 2017.)

Figure 8. Collisional deformation since ~155 Ma, when NAM first rode into the archipelago, welded into its westward-subducting plate. Progression of deformation is shown (A) in three time slices of cartoon cross sections through crust and mantle, and (B) in the eastward progression of dated faults (triangles) and folds (diamonds) in the western USA and southwest Canada. (A) At 160 Ma, arc magmatism above the westward-subducting Mezcalera Ocean, at the leading edge of North America (NAM), adds crust to the Insular Superterrane (INS) arc and lithosphere to the MEZ slab wall. Circa 155 Ma, the last of Mezcalera lithosphere is consumed between NAM and easternmost INS: NAM collides with INS

microcontinent, resulting in Nevadan deformation at the California margin and upward truncation of the slab wall (140 Ma panel). Further manifestations of this continent-microcontinent collision are deformation in the Omenica Belt of southern Canada, and deposition of the first west-derived sediments in the Western Canadian Sedimentary Basin, the Late Jurassic Passage Beds. As NAM is still being pulled westward (by intact trench segments in and out of the figure plane), subduction polarity at the collided segment is forced to flip, resulting in a new margin-hugging arc, including the Sierra Nevada batholith (SNB), which overprints the NAM-INS suture. Slab deposited by eastward (southern Farallon) subduction creates an east-dipping blanket (100 Ma panel) as the trench is forced westward in front of advancing NAM. Both north and south of the initial collision site, NAM continues to collide with microcontinental INS, resulting in widening Sevier deformation (Columbian orogeny in Canada), which is driven continually eastward. Map (B) shows this eastward and outward progression of deformation with dated faults and folds, using the same color-time conversion as trenches in (A), 20 m.y. per color increment.

Figure 9. Margin-parallel terrane translations based principally on paleomagnetic data from Late Cretaceous and Eocene strata. These data constrain the tomotectonic terrane reconstruction model of Clennett et al. (2020), which is modified in the figures. (A) Present-day terrane map shows the current locations of a half-dozen units that are very robustly constrained. The green/blue lines (with dates in Ma at nodes) represent spatio-temporal trajectories into the past of these units, back to where they were deposited, according to our Clennett et al. 2020 reconstruction. This reconstruction honors the constraints of the most solid paleomag sites, Carmacks & Mount Tatlow/Churn Creek, but Spences Bridge paleomag is not honored since it does not fully pass the fold test. Magnitudes of terrane offsets in the model are consistent with the paleomagnetic data. Trajectories are modeled in absolute coordinates relative to the lower mantle. The *main* BajaBC translations are implemented 70-50 Ma along the yellow line, which runs mainly through Intermontane terranes (and their left-behind correlatives in the Blue Mountains/U.S.). This Baja-BC fault line is necessarily speculative, but it must run inboard of all paleomag sites that show significant offsets (details in section 6.2). Accreted superterrane packages are colored as in fig. 7; additional pericratonic blocks are colored dark and light purple.

(B) 85 Ma snapshot reconstructing the assembly of Alaska. Tomotectonically inferred the northward sprint of Baja-BC, and its accretion to the arcs of future Central Alaska. These events occur on the Orcas microplate (MP), the space between the two old, stationary ANG (red barbs) and Farallon CR trenches (green barbs). The future Central Alaskan arcs (red) are gradually dislodged from their SW-ward subducting ANG slab as NAM overrides obliquely – the “Great Alaskan Terrane Wreck” of Johnston (2001). BajaBC (INS and western IMS in Canada) has arrived from the south along the yellow main shear fault and are now quasi part of the Orcas MP, separated from the NAM plate by the main fault (yellow line). Baja-BC passes *inboard* of, and unimpeded by, the CR Farallon trench, which still sits offshore. The Orcas MP is small and displaceable; as NAM pushes westward, Orcas is squeezed out toward the west or northwest, probably subducting into the area of the gray oval (a small upper mantle-slab overlying the CR slab, see text). Due to the small size of the plate, its disappearance can be very rapid, and the Baja-BC and Central Alaskan terranes follow along. As the Orcas seafloor subducts, the Farallon trench persists and makes landfall on NAM. Baja-BC and Central Alaska collapse against each other and against NAM, completing the assembly of Alaska. The angle between the yellow line (paralleling the NAM margin) and the ANG slab (red line) sets the angle of the future Alaskan orocline. Override and SW-ward subduction finishes ~55 Ma according to slab geometries. The offshore CR trench converts into the margin-hugging Cascades trench, closing off this northwestern passage for shuffling terranes.

Tomotectonics of Cordilleran North America since Jurassic times: double-sided subduction, archipelago collisions, and Baja-BC translation

Karin Sigloch & Mitchell G. Mihalynuk

Abstract

Tomotectonics uses deep mantle structure in order to hindcast paleo-trenches, by spatially superposing subducted lithosphere (slabs) imaged by seismic tomography with plate reconstructions at the surface. The two geophysical datasets combined make predictions about geologic events, specifically about volcanic arcs and their collisions with continents. The tomotectonic null hypothesis is simple, predictive and testable. It uses land geological observations for validation. We explain the method, with a clear conceptual separation of its hypothesis-generating stage (using geophysics and the hypothesis of vertical slab sinking) from its subsequent hypothesis-testing stage (using geological observations from accretionary orogens).

With the North American Cordillera as a case study, we generate a full suite of tomotectonic inferences on the slab assemblage that now occupies the mantle under North America to depths of 1800-2000 km. We reason why this assemblage originated as a completely intra-oceanic archipelago of paleo-trenches at a time of worldwide tectonic reorganization: around 200-170 Ma, when the Atlantic began to spread and the Pacific plate was born. An Archipelago is circumscribed by trenches that pull in seafloor from (at least) two sides: here, roughly from the east and from the west. North America was pulled westward by, and overrode, the westward-subducting arcs. These collisions since ~150 Ma caused the Nevadan and Sevier orogenies, and spawned the eastward-subducting arc that built Sierra Nevada Batholith ~120-80 Ma.

From ~110-50 Ma, the continent collided with the arc of future Central Alaska and with the Farallon arc of the Pacific Northwest, which sat offshore until ~90-50 Ma. Override of this double-sided arc pair enabled a range of collision styles, including the Baja-BC northward sprint and its accretion to Central Alaska. Tomotectonics infers large-scale northward displacement of Insular Superterrane since its accretion, which provides independent support for the “Baja-BC” hypothesis of paleomagnetism.

1. Introduction

The term “tomotectonics” refers to a set of quantitative reasoning tools for reconstructing the paleogeographies of regions shaped by subduction. Tomotectonics aims to account for all observations that record the processes of (paleo-)subduction, above and below the surface, and to reconcile them in a hypothesis-driven framework. Two types of observations play a primordial role in that they generate the predictions of the tomotectonic method, and they feature in its name: “tomo” (for seismic tomography of subducted lithosphere in the mantle) and “tectonic” (for plate tectonics). These are largely geophysical observations, which are linked by a null hypothesis about slab sinking that generates a shared, absolute spatial reference frame for slabs and plate motions.

Geological field observations play a different role: to test the tomotectonic predictions, and thus to reject or support the null hypothesis. Pertinent geological observations are made in accretionary orogens, which

are the surface products of the long-lived subduction processes recorded by the slabs. They contain the volcanic arc terranes that are directly and causally tied to the lithosphere that subducted. This paper applies the tomotectonic method to the North American Cordillera, inferring and evaluating its paleogeographies since Jurassic times, which turns out to be a natural limit of scope in the mantle and at the surface.

The strength of the tomotectonic approach is its particularly simple, strong working hypothesis, which describes the behavior of subducted oceanic plates once they have entered the mantle. With very few degrees of freedom, the hypothesis is highly predictive – and realistically falsifiable, the hallmark of a useful hypothesis. It does not follow that its falsification is easy in practice because the observational database of land geology is so incomplete. The essence of subduction is to remove its own traces from the surface into the subsurface. By contrast, the inventory of paleo-seafloor deposited in the mantle should be complete. That leaves the practical challenge of imaging it completely with seismic tomography, a domain where major progress has occurred over the past ~20 years (Earth Model Collaboration 2024, Hosseini et al. 2018, Pavlis et al. 2012).

The first, prediction-generating part of this study consists of Sections 2-4 (figures 1-6). Section 2 presents the relevant observations from mantle tomography and quantitative, global-scale plate reconstructions. Section 3 explains the tomotectonic working hypothesis of vertical slab sinking, which links the two data sets and renders them predictive. Section 4 carries out this predictive program by hindcasting paleo-trenches and their override sequences for North America.

Part 2 (Sections 5&6) examines these predicted arc building and accretion events in light of geological observations. The validation principle (Section 5) is that every slab in the mantle predicts a (paleo-)arc at the surface, which should correspond with a geologically observed arc of suitable age, spatial extent and composition (e.g., continental versus oceanic). Equally important, every geologically known arc should be paired with a plausible slab in terms of location and depth. Section 5.3 re-runs the tomotectonic override sequence of Section 4.4 in order to spell out its predictions for the paired, real-world arc terranes.

We have been able to identify only one set of slab/arc matches that leaves no orphaned arcs or slabs, and invokes no more complicated behavior than admitted by the tomotectonic null hypothesis (Sigloch & Mihalynuk 2013, 2017). It has generated significant debate because it predicts more intra-oceanic subduction and later accretion events (Late Jurassic to Cenozoic) for Cordilleran superterrane than more established interpretations (Monger & Gibson, 2019). On the other hand, the established interpretations have all been challenged from within geology as well (Moores 1970, Moores 1998, Johnston 2008, Hildebrand 2009, Schweickert 2015, Tikoff et al. 2023). Here we focus more on inferring large-scale transform motions from major structural breaks in the younger slab assemblage – pertinent to “Baja-BC” displacements mostly between 90-50 Ma (Irving 1985, Kent & Irving 2010, Tikoff et al. 2023). Such displacements obscure terrane accretions that pre-date them and are seemingly at odds with concurrent continental arc construction (Cowan et al., 1997). However, the mantle is very informative and provides a geometric solution to the Baja-BC conundrum.

The reasoning of Section 5 provides the skeptical reader with a template for proposing and evaluating alternative sets of slabs-arc pairings that satisfy the same observations and simple null hypothesis – or for consideration of what level of mantle convection complexity might need to be invoked in order to envisage a different interpretation of the surface geology, and whether such complexity yields a predictive working hypothesis.

Section 6 raises discusses how all collisions types in the Cordillera were shaped by double-sided subduction in one form or another: from the early heads-on collisions in the U.S./Sierra Nevada segment,

to the late, very oblique collisions of Central Alaska and Baja-BC. Section 7 provides synopsis and considerations for future work.

2. Observations for a tomotectonic reconstruction of Cordilleran North America

Tomotectonics makes spatial and temporal superpositions of two types of structures that are observable essentially by geophysical means:

- 1) The 3-D geometries of subducted oceanic lithosphere in the mantle ("slabs"), obtained from seismic tomography.
- 2) Quantitative reconstructions of plate motions across the earth's surface over time, mainly based on remnant magnetism of extant seafloor.

For North America (NAM) a superposition of slabs and plate motions for the past ~170 million years (Ma) is shown in Figure 1, which serves as a visual roadmap for this study. The translucent patches outline mantle regions (volumes) where subducted seafloor is observed at certain depths between the surface (0 km) and 1800 km. A first-order observation is that slab distribution is uneven, and that large regions of the mantle do not contain slab at any depth.

Outlines of the NAM west coast trace the continent's westward drift over the past 170 Ma, as reconstructed by the Global R absolute reference frame (Torsvik et al. 2019). If in a thought experiment, a resident of the U.S. west coast could be transported 130 million years (m.y.) back in time, the reconstruction of figure 1 hindcasts that they would end up in a present-day latitude and longitude signaled by the "130 Ma" coastline, an absolute position that is presently occupied by the *east* coast of the U.S.

2.1 Tomographically imaged slabs

Figures 2 and 3 render all slabs (or rather, seismically fast P-wave anomalies) in the teleseismic P-wave tomography model of Sigloch (2011), down to ~1800 km depth in the mantle (where this regional model loses resolution). Mantle imaging under North America made a quantum leap in the wake of the USArray Transportable Array deployment across the (western) U.S., when ~400 broadband seismometers rolled across the contiguous U.S. between 2004-2013 (). In more recent models, including global models that image deeper (Hosseini et al. 2018), the resolution under North America remains driven by the USArray data set. Other regional tomographies of North America can be inspected at the portal of (Earth Model Collaboration 2024). The massive slab complexes to be discussed are well delineated in practically all post-USArray tomographies. Imaging differences or uncertainties persist mainly in the shape of less massive, upper-mantle slabs. Examples concern the spatial continuity of recently subducted Cascadia (Farallon) slab (see review of Pavlis et al. 2012), or the vertical delineation of old, stable continental lithosphere against slab in the transition zone below it (both are seismically fast).

Figure 2 renders two 3-D oblique views of the slab complex into which the Farallon (Juan de Fuca) slab subducts today. Slow seismic anomalies, which are proxies mainly for hotter-than-average mantle (e.g., Yellowstone), are not rendered but can be inspected in Sigloch (2011). We prefer these 3D iso-surface renderings to the more commonly seen 2-D depth slices ("red-blue" maps) because vertical continuity of structure is particularly important in tomotectonics. The disadvantage of oblique views is that their 3-D

content cannot always be presented satisfactorily on 2-D paper. As a compromise, we show the same 3D renderings in “map view”, with the virtual camera pointing vertically down – as in figure 3a, or up as in fig. 3b. With color as a proxy for depth, such “3-D map views” convey the vertical connectivity of structures, and easily tie to surface map overlays. The “inside-out” map view of fig. 3b renders the deepest (red) slabs in the foreground, unobscured by the blanket of shallower slabs. The deepest slabs (1100-1800 km) are very steep, linearly elongated, and highly structured. We call them “slab walls”.

To get oriented, we encourage the reader to find the slabs cartooned in fig. 1 in the 3-D renderings of figs. 2 and 3.

That seismically fast anomalies (below lithospheric depths) represent subducted lithosphere has become a quasi-certainty as imaging resolution has improved over the decades. Lots of lithosphere is expected under North America from its subduction history, and at least recently subducted slab should remain topographically visible. Indeed, fast anomalies are now unfailingly imaged in the upper mantle below subduction zones (e.g., the purple slab level beneath Cascadia in fig. 2). The fast anomalies coincide with the band of seismicity produced by the slab, which ground-truths the tomographic detection. The imaged anomalies usually continue below the deepest earthquake depths, and this satisfies *a priori* expectations from geologic or plate tectonic records of longer subduction histories (at least 180 m.y. in the case of the northern Farallon slab of fig. 2). Finally, there is no plausible alternative for what the fast anomalies might otherwise represent.

2.2 Quantitative plate reconstructions

The primary constraints on quantitative plate reconstructions come from paleo-seafloor spreading ridges. Their spreading histories are recorded as isochrons (“stripes”) of alternating seafloor magnetization, which in principle permit very detailed and accurate reconstructions of relative plate motion circuits as long as plates can be linked through paleo-spreading ridges. The activity of trenches destroys these records by subducting the magnetized seafloor. Hence isochron-based reconstructions do not reach back beyond 100-200 Ma, but for North American reconstruction, the situation is very favorable. We require mainly the (completely preserved) Atlantic spreading record, which is completely preserved back to Pangean times (>170 Ma, Müller et al. 2008), and we have the added bonus of an exceptionally long (>180 Ma) record of Farallon-Pacific spreading in the Pacific basin (Engebretson et al. 1985).

Seafloor isochrons only permit reconstructing the paleo-plates’ motions *relative to each other*. It is crucial to appreciate that the reconstruction of fig. 1 is delivered in *absolute* coordinates relative to the lower mantle. The lower mantle is chosen as reference because it is the most slowly changing among the earth’s layers, moving 1-2 orders or magnitude more slowly than tectonics plates. The absolute tie of relative plate circuits to the lower mantle is achieved via intraplate hotspot tracks: the entire lithospheric shell of the earth must be translated relative to the deeper mantle over time, such that in the reconstruction for time T, all seamounts dated to time T in the various tracks come to overlie the *present-day* positions of their generating hotspot volcano. The mantle plumes presumed to create the volcanic hotspot tracks are expected *a priori* to originate as upwellings from the lowermost mantle. The reasoning is that hotspot tracks empirically yield the best available proxy for the quasi-stationary lower mantle. Indeed, the set of (Indo-Atlantic) hotspots is observed to have moved only very slowly relative to each other (<10 mm/yr) (Morgan 1983, O’Neill et al. 2005). The simplest explanation is that the hotspots do not move relative to the medium in which they are anchored, i.e., the lowermost mantle. The specification of “Indo-Atlantic” hotspots is important because North American paleo-positioning in fig. 1 is achieved relative to this well-

behaved, near-stationary set of hotspots of the Pangean hemisphere. Pacific hotspots, whose stationarity is more questionable (Wessel & Kroenke 2008) do not enter any of our reconstruction arguments.

Tomotectonic reconstruction uncertainties have been quantified by Sigloch & Mihalynuk (2013), Supplementary Information. They are a combination of uncertainties in relative plate circuits, absolute reference frame, imaging uncertainties, and uncertainties about the shapes of the paleo-margin over time. Before ~120 Ma, the uncertainty in absolute reference frame dominates (loss of hotspot track constraints), i.e., the “120-Ma margin” and the “110 Ma margin” might be indistinguishable in their absolute positions (whereas the increment in westward step between them is much more certain, from isochron spacing). At 150 Ma, this absolute positioning uncertainty is >20 m.y., and for times more recent than 100 Ma, it is ~5-10 m.y. These numbers need to be kept in mind when interpreting the paleo-coastlines in fig. 1. In addition, coastlines change shape as terranes accrete and shuffle along the margin (in fig. 1, according to the model of Clennett et al. 2020). Coastline shape uncertainties are significant and difficult to quantify, due to lack of constraints on the original shapes of the accreted microcontinents (Sigloch & Mihalynuk 2013). They are probably comparable to the absolute positioning uncertainty.

3. The tomotectonic null hypothesis of slabs settling vertically

If a present-day resident of the U.S. eastern seaboard were able to drill 1000 km vertically into the lower mantle, they would hit the orange slab shown in figure 1. If the resident moved to the west coast and then travelled back to 130 Ma on the west coast, would they also drill into the mantle – would they also hit the orange slab? This question is non-trivial. The paleo-seafloor contained in the slab might not have subducted yet at 130 Ma, in which case the answer would obviously be “No”. Assume the seafloor had already subducted, or was in the process. The time traveler’s drill would then hit the slab *if that 130-Ma slab occupied the same latitudes and longitudes of figure 1 as the present-day orange slab*. In other words, “Yes” if the slab sank vertically, without lateral displacement relative to the lower mantle (where it is observed today). This kind of simple, vertical sinking into the lower mantle is the null hypothesis of tomotectonics.

3.1 Predictive power of the hypothesis

No lateral displacement of subducted lithosphere once it has entered the mantle – this hypothesis makes strong predictions about the paleo-surface. It predicts that the trench through which the orange slab entered the mantle was located at the same absolute latitudes and longitudes occupied by the slab today. No other method provides such straightforward predictions of paleo-trench geometries. It is also obvious to hindcast the absolute locations where no trench was ever present: those are the slab-free areas in fig. 3.

Joint consideration with the plate reconstruction multiplies the predictions. Recall that the west coast in fig. 1 is reconstructed relative to the lower mantle. Under our null hypothesis, the (lower-mantle) slabs of fig. 1 have not moved laterally since entering their trenches. Hence the slabs and the continent are shown in the same, lower-mantle reference frame, their absolute coordinates directly comparable. The slabs map out paleo-trench locations (vertically above them), although we need more information to determine when each trench was actively depositing slab.

Under this hypothesis, the passage of reconstructed North America across the slab-scape in fig. 1 directly translates into a paleo-movie of the continental margin riding into a network of subduction zones. The trenches can only be active if the continent was not occupying their positions. By the end of the movie (0 Ma), all slabs must have been deposited in their observed positions, vertically below a network of paleo-

trenches, the positioning of which must respect plate geometries and other plate tectonic rules. For example, no slab can be deposited under the eastern half of the U.S. after ~80 Ma, when the continent is already overlying this region in fig. 1, meaning no trench and arc can be assigned to this region. Between ~170-150 Ma, the west coast traverses a slab-free zone, hence a trench along the west coast is not admissible for those times under the vertical sinking hypothesis. From ~150 Ma onwards, certain latitudes of the west coast overlap slab provinces (dark orange & light green in fig. 1), which means that a margin-hugging (“Andean-style”) trench at those times and latitudes is possible. Alternatively, the slabs might have been deposited earlier, into an intra-oceanic trench, west of the west coast.

Figure 4 spells out the consequences of the vertical sinking hypothesis for the slabs produced. Crucially, vertical sinking is capable of producing the entire range of observed slab geometries. Vertical slabs result from vertical sinking under a stationary trench. Dipping slabs result from vertical sinking under a migrating trench, dip angle being determined by the ratio of trench velocity and sinking velocity. Slabs have the thickness of lithosphere if they sink away as quickly as more material enters the trench. If sinking is not rapid enough, the slab needs to thicken, probably by folding, as cartooned. Such “traffic jam” conditions prevail in most present-day subduction zones Cerpa et al. (2022): plate convergence is typically 50-100 mm/yr, of which only one half to one quarter can be accommodated by slab sinking away and/or the trench moving laterally away.

3.2 The vertical sinking hypothesis pertains to thickened slabs

Is the vertical sinking hypothesis plausible, or is it grossly simplistic? That depends on the length scale considered. In tomography models, slabs appear ubiquitously thickened from the mantle transition zone down. A sheet of subducting lithosphere is <100 km thick, whereas, the slab walls of fig. 3 measure 300-600 km across their narrow horizontal dimension, and the FS slab is >300 km thick in z-direction. The only “thin” slab is the FN (Gorda) slab on its first 200-300 km beyond the Cascades trench. Hence the tomotectonic null hypothesis needs to only concern itself with thickened slabs. The lower row of fig. 4 ($K_r=1$) is basically not observed by tomography, consistent with observations by Cerpa et al. (2022) of excess trench convergence at the surface.

The more massive a slab, the more nearly vertically it is expected to sink because gravity is the only primary force driving mantle convection. Slabs walls are among the most massive slabs in the mantle (and of a shape streamlined for vertical sinking). Lateral displacements, such as plate motions at the surface, or “mantle wind”, arise only in order to close the flows between downwelling and upwelling limbs of a convection cell. Massive slabs are actively driving the downwelling, hence should be least susceptible to be passively entrained sideways.

A strong observational indicator for vertical settling is the prevalence of slab-walls in fig. 3b. The deepest slabs all have this shape. Their simplest explanation, cartooned in fig. 4, is vertical settling beneath a stationary arc-trench system. The alternative of non-vertical sinking (plus a non-stationary trench exactly compensating for the non-vertical sinking) seems contrived, especially considering the massive slab volumes that would need to move around laterally.

3.3 Lateral uncertainties on vertical sinking

The laying down of slab folds (as cartooned in fig. 4, top row) almost certainly introduces non-vertical sinking in the uppermost mantle, on the length scale (amplitude) of the lateral folds, which is a few hundred kilometers. The relevant physics are those of a viscous thin sheet (lithosphere) encountering a

(semi-)rigid backstop (the lower mantle)(Ribe et al. 2007) – sometimes observed while pouring cake batter or honey. For paleo-reconstruction, these lateral folds introduce a commensurate uncertainty about where the paleo-trench ran above a slab wall: centered, shifted towards the trench, or away from it? We may yet learn the answer but for the moment have to admit an arc placement uncertainty of 200-300 km. Hence we call slab sinking “vertical” if it is observationally indistinguishable from vertical to within a few hundred kilometers lateral uncertainty.

If NAM approached a slab wall at 20-30 mm/yr, 200-300 km of lateral trench uncertainty translates to a timing uncertainty of ~10 m.y. as to when exactly the margin encountered the trench above this slab wall. This is not insignificant and needs to be kept in mind. (Uncertainties on the exact shape, especially westward-extent, of the margin tend to be similarly large, see SI of Sigloch & Mihalynuk (2013).)

In summary, the tomotectonic null hypothesis is that (thickened) slabs observed in the lower mantle and transition zone sank vertically after entering their trenches (with lateral uncertainties of a few hundred kilometers). This is plausible *a priori*, and supported by observed slab geometries. Despite these promising indications, we do not *assume* vertical sinking in what follows. Vertical sinking remains a hypothesis – it generates predictions, which have to hold up to attempts to falsify them.

3.4 Uniformity of slab sinking

There is no need to hypothesize further specifics about slab sinking, and in particular no stipulation of any sinking rates *a priori*. If deeper slabs are found adjacent to shallower slabs, there is an intuitive expectation that the deeper slabs subducted earlier, because all slabs sank through essentially the same medium. We will occasionally use this expectation to arbitrate between two explanatory alternatives (e.g., for slab W), but there is no need to elevate this expectation to a part of the hypothesis. The slabs will turn out to obey this principle automatically.

There are many opportunities to *estimate* sinking rate from the slab geometries – we will encounter some, and proper quantifications can be found in Sigloch & Mihalynuk (2013) and Mohammadzaheri et al. (2021). These estimates indicate that the slabs sank at ~10 mm/yr (plusminus 2 mm/yr), more or less everywhere across the Americas, which is a remarkable result in terms of uniformity. It has led to widespread misconceptions that tomotectonics assumes or imposes a sinking rate arbitrarily. To counter this impression, the present study will make very little mention of sinking rate, leaving it largely implicit in the tomotectonic observables. An explicit sinking rate is only needed when making an actual tomotectonic movie, where slabs grow at a rate commensurate with plate advances (e.g., Sigloch & Mihalynuk 2017) – in which case ~10 mm/yr is the only value that “works” with vertical sinking.

We finish with the single most striking observation that suggests a basically uniform sinking rate: the deep ends of the slab walls of figure 3b all reach to 1800-2000 km depth, across the entire study domain. (The regional tomography of figs. 2 & 3 loses resolution around these depths, but global-scale tomographies confirm 1800-2000 km as the deep ends of the slab walls (Hosseini et al, 2018). Below 1800-2000 km, copious volumes of slab are present into the lowermost mantle, but in geometrically different arrangements. This suggests a comprehensive and relatively sudden reconfiguration of paleo-trenches across the area, *plus a constant sinking rate across the domain*, otherwise the slabs that were deposited after the reconfiguration event (and which are the subject of our study) would not all have reached the same depth of ~1800-2000 km. What was this event? Section 4 will yield the answer without reference to a sinking rate, but at 10 mm/yr, a slab depth of 1800 km translates to a mantle entry time of 180 Ma. This is the

time when Central Atlantic opening started appreciably, setting North America on its westward drift, and also when the Pacific plate (and possibly the Farallon plate) were born – indeed a major reconfiguration that may have fundamentally reset paleo-Pacific subduction zones. These observations are all mutually consistent – supporting uniform slab sinking, as well as clear correspondences between deep mantle structure and known, major surface events. The slab breaks at 1800-2000 km depth thus provides a natural limit for the scope for our reconstruction. The older archipelago beneath the current one is not as sharply resolved by tomography, and the uncertainties on absolute paleo-positioning at the surface (in absence of hotspot tracks) become unworkable beyond Jurassic times.

4. Tomotectonic reconstruction of North America

4.1 A western and an eastern slab complex under North America

We are ready to execute the predictive stage of tomotectonics. One by-product will be figure 5, which makes paleo-trench predictions by “transcribing” the slab-scape of fig. 3 using the tomotectonic null hypothesis. The tomography model is sliced into horizontal maps in depth increments of 100 km. At each depth, a paleo-trench line is drawn above every slab present, and colored according to the depth-to-color scheme of fig 3. For slab walls, it is easy to draw the line (centered inside the narrow slab). For the almost vertical slabs, the lines change little with depth, resulting in tightly clustered lines in fig. 5. For dipping slabs, the transcription is subject to larger uncertainties, and paleo-coastlines or interpolations may also be used, as will be explained.

The assemblage of slabs under North America clearly separates into two groups (figs. 1 & 3): a Western Slab Group comprising slabs CR, W and FN; and an Eastern Slab Group, comprising slabs MEZ, ANG, and FS). Slabs within each group are spatially connected, and separated from the other group by slab-free mantle.

Figs. 1 and 3a show a small overlap between the two slab groups (easternmost CR and westernmost FS), but only laterally, not in depth. This does not violate the vertical sinking hypothesis: the area hosted two different trenches, at different times. The older trench deposited the deeper CR, and the more recent trench deposited FS. The deepest slabs in both groups are slab walls (MEZ, ANG, deep CR), and they all reach to the same depth of 1800-2000 km (magenta color level in fig. 3b).

4.2 Tomotectonic reconstruction of the Western Slab Group (northern Farallon slabs)

The three slabs of the Western Group (FN, CR, and W) are jointly rendered in fig. 2. The 3-D oblique views make clear that the three slabs really form a single system, sloping down to the east. The view angle of Fig. 2a emphasizes spatial continuity, making clear that the three slabs really form a single system that slopes down to the east. By contrast, the view angle of fig. 2b highlights intra-slab breaks and structural divisions. Slab W is seen to be a completely separate fragment in fig. 2b, but clearly in a spatial correspondence with CR in fig. 2a. The separate definition of FN and CR in fig. 1 may seem arbitrary from fig. 3a (FN is the upper-mantle part of the whole, corresponding roughly to the purple, light and dark blue levels), but in fig. 3c we see that this upper-mantle slab is almost “floating” freely, due to gaps towards the slab components surrounding it.

For visual clarity, fig. 2 masks out certain slab parts by comparison with fig. 3, which renders *all* seismically fast structure (below 400 km depth). Fig. 2 omits the deep slab fragment west of today’s west

coast. It also masks out an upper-mantle slab that strikes east-west under southern Saskatchewan, Alberta and B.C. (dark blue in fig. 3a), and which does not participate in the sloping continuity of the Western Group but rather seem to rest on top of it. (We later return to this slab as the speculated Orcas slab.)

4.2.1 FN slab – northern Farallon slab in the upper mantle, margin-hugging trench

Below the present-day coastline of the Pacific Northwest in figs. 2 and 3, shallow slab is imaged beneath the active Farallon (Juan de Fuca) subduction, but neither north nor south of it. This provides a first reassurance that the tomography “works”: a slab is imaged below a confirmed (present-day) subduction zone, no slab is imaged below adjacent non-subduction zones.

For depositing the upper-mantle slab FN to the east of the trench, a margin-hugging trench is the only plausible scenario i.e., a continuation of the present-day situation into the past. The continental margin gradually traversed FN slab over the past ~70 m.y. (fig. 1), and FN slab gets shallower to the west (fig. 2a). Westward shallowing is consistent with deposition of FN under a westward migrating (marginal) trench, so that easterly FN is deeper because it had more time to sink. In fig. 4, FN most resembles the folded slab in the top row, second from the right.

“FN” stands for Farallon North. Near the trench, the slab can only represent Farallon lithosphere because the Farallon (Juan de Fuca) plate is subducting into it today. Magnetic isochrons on the Pacific plate trace the growth of the (northern) Farallon plate from ~180 Ma to 0 Ma (Atwater 1989, Engebretson et al. 1985), spreading towards the Western Slab Group. Since these slabs represent the paleo-trenches closest to the reconstructed Pacific-Farallon spreading ridge over time (e.g., Engebretson et al. 1985, Seton et al. 2012), (and indeed Farallon plate is still subducting into this slab today), the plate must have subducted into FN in the past as well.

In summary, FN holds Farallon lithosphere, and today’s Farallon trench is built on the continental margin. The margin’s eastward progression back into the past in fig. 1 matches the FN slab’s eastward down dip: everything points to a margin-hugging trench in the past as well.

4.2.2 CR slab – northern Farallon slab in the lower mantle, intra-oceanic subduction

At first glance, lower-mantle CR slab (turquoise levels and below in figs. 2&3) seems to smoothly continue the downward dip of FN slab (with a margin-hugging Farallon trench as the explanation), but there are serious problems with this proposal. With increasing depth, CR slab appears increasingly spread-out laterally in fig. 2a. The reason is that deep CR is no longer dipping east. Rather it has steepened into a slab wall and also rotated counterclockwise compared to FN and the coastline, with its long axis striking NW-SE (especially clear in Fig. 3b). If the deep CR dips at all, it is to the west, in the “wrong” direction for subduction beneath a west-migrating continental margin. Deposition of the voluminous slab wall portion of the CR required a stationary trench striking highly oblique to the coastline (fig. 1). At yellow/green depth levels in figs. 2 and 3, the CR slab looks segmented and complex, including a detached fragment W – again no good match to the paleo-coastline.

CR is much more voluminous than FN, requiring a trench that dwelled in the area, but the coastline did not dwell: by >80 Ma, it shows no overlap with CR slab in fig. 1. The northern Farallon plate was spreading since >180 Ma, so the margin in fig. 1 leaves the CR slab 100 m.y. too early. It subsequently traverses the slab-free zone to the northeast of CR, which for tomotectonics implies no trench along the

margin. Finally, an isolated slab as deep as CR is present just offshore the present-day west coast in Figures 3a and b – further west than the margin ever came.

The inevitable conclusion is that CR (and the deep western offshore slab, which is rendered in fig. 3 but not fig. 2) cannot have been deposited into a margin-hugging trench, unlike FN – prior to 80 Ma (roughly), the northern Farallon trench must have sat offshore the NAM west coast. Jointly, FN and CR are voluminous enough to account for the observed 180 m.y. of northern Farallon spreading and subduction.

Hence by coincidence, FN is not just the upper-mantle part of the northern Farallon slab, but also the part that was deposited by an Andean-style trench. CR is the lower-mantle Farallon slab, deposited by an intra-oceanic trench. The geometric complexities at intermediate depths of CR presumably reflect the prolonged, oblique override of by NAM <80 Ma that gradually “accreted” the Farallon trench. This tomotectonic prediction of an offshore Farallon trench in the Pacific Northwest >80 Ma has many implications, including that Baja-BC terranes could have shuffled northward *inboard* of this trench (section 5).

In terms of trench lines for fig. 5, the deep slab wall of CR is easy to transcribe (compare to fig. 3b). For the dipping FN slab, paleo-coastlines were equated to trench lines since a margin-hugging trench has been inferred. The intermediate-depth (turquoise) trenches above the fragmented, rotating slab were drawn as best guesses/interpolations, and they almost certainly are too simplistic. The strikes of trenches drawn above W are guesswork since the slab lacks a clear strike, and we do not understand its functioning relative to CR. The very deepest (magenta, grey) levels of CR are also guesswork – were the two separate slab walls originally connected into one long, E-W striking slab (Sigloch & Mihalynuk 2013)? The strike and shape of the westernmost, offshore fragment is not well imaged. The overall complexity of the Western Group is real and not an imaging shortfall – much of its information remains to be deciphered.

4.3 Tomotectonic reconstruction of the Eastern Slab Group

4.3.1 FS slab – southern Farallon slab in the transition zone and lower mantle

FS, MEZ and ANG slabs comprise the Eastern Slab Group consists of FS, MEZ and ANG slabs. FS should have subducted most recently due to its more westerly and shallower position than MEZ and ANG. The paleo-coastline of fig. 1 traverses FS from ~130 Ma (± 15 Ma) to ~75 Ma (± 10 Ma?), so deposition must have concluded by the later date. The slab occupies the same depths as lower FN and intermediate CR, for which we have inferred similar dates.

FS slab features a linear, sharp truncation towards its southwest, where the mantle becomes slab free. This truncation (yellow line in fig. 1, the “Big Break”) approximately coincides with the strike of the paleo-coastline at 75 or 80 Ma. The simplest explanation for this coincidence is that the FS trench was built on the margin, and that (vertical) deposition into this marginal trench suddenly stopped at 75-80 Ma. The slab’s elongation in WSW-ENE direction, which is the direction of margin advance, likewise suggests that FS was deposited beneath the migrating NAM margin.

In fig. 3b, FS slab tends to deepen toward the east (and the south) generally speaking, albeit irregularly. This also points to deposition below the migrating margin: easterly FS slab regions have had more time to

sink. The gentle overall dip of FS suggests that its trench migrated relatively rapidly: FS slab geometry best corresponds to the upper right case in fig. 4, where the slab flattens in and below the transition zone.

An eastward-subducting, margin-hugging trench during Cretaceous times, just south of the northern Farallon system, must be another Farallon trench. The reason is cartooned in figure 6. When Farallon-Pacific (FAR-PAC) spreading had just started (time 170 Ma), the associated spreading ridge segment is short (as recorded by Pacific isochrons), so the CR slab is wide enough in latitude to account for the young Farallon plate (fig. 6a). But over Cretaceous times and by 80 Ma (fig. 6b), the FAR-PAC ridge had extended southward, too far to be accounted for by CR slab only – since CR did not grow southward. Hence an additional Farallon trench segment should have developed to the south of CR. FS slab exactly mirrors the lengthening of the Farallon spreading ridge by a commensurate lengthening of the trench: FS starts out very narrow at the 130-Ma coastline but widens southward to underlie much of the U.S. and Mexican paleo-margins by the time the 80-Ma coastline reaches the Big Break.

In summary, all aspects of FS point to subduction of the southern Farallon plate over the Cretaceous period (roughly 130-75 Ma), beneath the NAM margin. Fig. 6b sums up Farallon subduction shortly before the Big Break: beneath the NAM margin of Mexico and California, but still offshore in the Pacific Northwest.

4.3.2 Slab-free window between the present-day margin and FS slab

Now consider the significance of the slab free area southwest of the Big Break in fig. 1, extending from FS slab to the current southern California and Mexican margins. South of the northern Farallon/Cascadia trench, a dextral transform plate boundary runs along the *present-day* margin (the San Andreas system). From Pacific isochrons, Atwater (1970) inferred this transform system back to ~30 Ma, to the reconstructed “landfall” of the PAC-FAR spreading ridge on the margin.

Tomotectonics can diagnose the existence of this same transform from the absence of slab beneath the present-day margin (so it is not a trench; and a continent-ocean boundary cannot be a spreading ridge either). However, according to figure 1 the slab-free window extends eastward from the coast not only to the 30-Ma paleo-coastline, but all the way to the Big Break, which corresponds to the ~75/80 Ma coastline. Hence tomotectonics hindcasts that a transform plate boundary has held sway along the Californian and Mexican margin since ~75 Ma, when the margin-hugging southern Farallon (FS) trench suddenly shut down in the Big Break event.

Slab W (traversed by the coast ~20-50 Ma) might signal a localized, temporary interruption (by subduction) of this transform regime, but it is unlikely. We noted that slab W is deep and blends into the overall geometries of CR, hence likely represents older events. If indeed slab W does not interrupt the subduction-free period, then the current San Andreas regime along the margin is in full spatial and temporal continuity with the transform regime of ~50-90 Ma that was inferred by rock paleomagnetism in order to transport the Baja-BC microcontinent northward (Kent & Irving 2010). This is a straightforward consequence of the wide slab-free window combined with the vertical sinking hypothesis.

4.3.3 MEZ and ANG slab walls

MEZ slab is among the longest and most voluminous slabs in the whole mantle. It is a gigantic slab wall that runs from northeast Canada to Florida under the NAM eastern seaboard, and from there on to Peru.

MEZ wall is >1,000 km “high” under Florida (occupying depth levels ~1800 km to ~800 km in the mantle column), but only ~300 km “high” under Nova Scotia (occupying ~1800-1500 km depth).

MEZ lies in spatial eastward continuation of the southern Farallon (FS) slab, and continues the eastward-deepening trend, although at a dramatically steeper angle than FS. The intuition might thus be that MEZ represents Farallon plate older than FS. Tomotectonics indicates that this cannot be the case.

The deposition of a voluminous, linear slab wall requires a trench that remains stationary above MEZ for a long time (fig. 4, top row, second from left). By contrast, the paleo-coastline in fig. 1 marches right across MEZ (and ANG) in fig. 1, without dwelling on the slab and without showing any correspondence with the slab’s shape. In reverse time, NAM leaves behind FS slab by ~130 Ma. By 150 Ma, the margin leaves behind the eastern promontory of MEZ slab wall and traverses only slab-free mantle until 170 Ma – the temporal limit of our study, when the east coast has reunited with Pangaea, the Central Atlantic is closed (see fig. 6a).

The swift and oblique march of the west coast across MEZ means that a *margin-bugging* Farallon trench could not have deposited the slab wall by vertical sinking. What about a stationary, offshore Farallon trench, as observed in the case of CR? The problem with eastward (Farallon) subduction into MEZ is that it would prevent NAM from moving westward, away from Pangaea, between 170 Ma and the moment it reaches MEZ (which is ~150 Ma at the MEZ promontory, and later further south). The slab-free zone between MEZ and NAM at 170 Ma is occupied by seafloor at the paleo-surface, and this seafloor must subduct in order to let NAM move westward. The only slab available to subduct into is MEZ, which means *westward* subduction of the seafloor between Pangaea and MEZ, into MEZ trench.

Hence MEZ could not have hosted an eastward subducting trench at the same time, meaning no Farallon trench, not even an intra-oceanic one. This is the decisive argument against MEZ as a Farallon slab. Westward subduction into MEZ solves other problems: the huge latitudinal extent of MEZ does not match the short isochron segment of FAR-PAC spreading ridge recorded for Jurassic times (fig. 6a). The FS slab, narrowing then disappearing to the east, already explains the history of southern Farallon growth.

By contrast, the north-south extent of MEZ is of the correct length and strike to let all of North America break free from Pangaea at once, and to start moving west ~170 Ma. The northern MEZ segment from Nova Scotia to Florida closely matches the Central Mid-Atlantic spreading ridge, in length and strike, and from 170 Ma to today. The situation is cartooned in fig. 6a, which highlights (in blue) the seafloor west of NAM that needs to subduct into MEZ (and ANG).

Fig. 6a that ANG slab served the same role as MEZ, enabling NAM to move west. MEZ trench pulled on the NAM margin at U.S. and Mexican latitudes, whereas ANG pulled on the B.C. margin. As required for this functioning, ANG slab wall is spatial NW-ward extension of MEZ, is very similar in character. ANG strikes very oblique to the paleo-margin, and it reaches very far west. This means that the margin took a very long time to override ANG slab – in fig. 6b, its trench is still pulling on the northern margin at 80 Ma, when MEZ has long been overridden.

4.4 Chronological sequence of archipelago override

Pulling all tomotectonic inferences together, we play forward the “movie” of continent-trench collisions, using figures 1, 3, 5 & 6. All trenches start up around the same time (same depth of ~1800-2000 km), while NAM is still with Pangaea, i.e., sometime before 170 Ma (fig. 6b). All trenches are originally intra-

oceanic in the proto-Pacific basin west of Pangaea, where they are free to remain stationary and to build the observed slab walls MEZ, ANG and CR.

MEZ and ANG trenches are exerting a westward pull on the NAM plate, whose western plate boundary is not the continental margin but an ocean basin (“Mezcalera-Angayucham Ocean” in fig. 6a). From ~200-170 Ma, the Central Atlantic rifts along a line parallel to northern MEZ slab. Central Atlantic rifting transitions to proper spreading ~170 Ma (Atlantic isochrons, e.g., Seton et al. 2012). The Atlantic opens at the expense of the Mezcalera-Angayucham Ocean, which narrows by westward subduction into MEZ and ANG slabs.

Around 155 Ma, the NAM west coast at U.S. latitudes starts to collide with the northern MEZ trench, under-riding the MEZ arc and deforming the margin (orange barbs in fig. 1). The collision gradually spreads in latitude as broader swaths of MEZ arc (and later ANG arc) are overridden (fig. 1, coastlines at 130, 110 Ma). The gradual override of northeastern MEZ slab ~155-110 Ma is recorded by the westward shallowing slab “ramp” it forms in fig. 3a: under the 150-Ma paleo-coastline, the slab had 150 Ma to sink since the end of subduction, and its upper truncation now lies ~1500 km deep (red level of the 3-D isosurface in fig. 3a); under the 110 Ma-line, its shallowest part lies 1100 km deep (yellow level) and has been sinking for 110 m.y. (This ramp is among the best opportunities to estimate slab sinking rate.) In fig. 5, the slab ramp translated to trench lines on northern MEZ “retreating” westward, from pink to red to yellow levels: no more trench where the Mezcalera Ocean has disappeared.

At U.S latitudes, subduction cannot cease with the consumption of all Mezcalera Ocean lithosphere because NAM continues to be pulled westward, by still-active northern ANG and by southern MEZ trenches. NAM is pulled into the area presently underlain by eastern FS slab, and the ocean lithosphere occupying this absolute position is forced beneath the advancing U.S. west coast, depositing FS slab. Hence subduction polarity flips along the California/Mexico margin: NAM margin turns into the overriding plate (green barbs in fig. 1), with Farallon plate subducting underneath it. MEZ and ANG trench segments shrink while FS trench grows along the margin. CR trench (northern Farallon) sat in the same stationary, intra-oceanic position the entire time.

At 80 Ma (fig 6b), these override events have run their course and things are about to change. The southern Farallon (FS) trench on the margin abruptly shuts down ~80/75 Ma and will never be re-established (Big Break of FS slab). A transform system takes over that evolves into the present San Andreas transform (slab-free corridor). The reason for this shutdown of the continental arc is not obvious, perhaps related to the beginning, oblique collision of NAM with northern Farallon (CR). At the end of a protracted override (fragmentation of upper CR slab), the seafloor that remained between CR trench and NAM in fig. 6b has been squeezed out and the northern Farallon trench has “accreted” (by ~50 Ma). It continues as the margin-hugging Cascades trench that is still active today (FN slab).

In the far north, ANG arc is under-ridden by NAM very gradually and obliquely into Cenozoic times, always by westward subduction. Once ANG subduction is completed, the northern margin turns into the transform system that continues to the present day.

5. The match between tomotectonic arcs and geologic arcs

So far, we have used only the tomotectonic observables of slab geometries and quantitative plate reconstructions for making the paleogeographic inferences of Section 4; these are linked together by the

null hypothesis of slabs sinking in place. Geological observables remain untapped and an independent data set for testing the tomotectonic hypothesis and its predictions.

The principal link for hypothesis testing is the volcanic arc, which is an inevitable surface manifestation of any subduction zone. Tomotectonics hindcasts absolute paleo-arc locations. If the tomotectonic method works properly, every paleo-arc predicted from slab observations should have an actual counterpart in the accretionary orogen. The converse is equally important: every geologically observed arc should be matchable to a suitable “tomotectonic arc”, that is, to a slab.

Figure 7 shows the large-scale assemblage of arc terranes since ~170 Ma that need to be explained along the present-day west coast of North America (left part of the map). Figure 7 also schematically reconstructs the paleo-arc terranes above their matched slabs and paleo-trenches. The chosen set of slab/arc matches will arguably yield the “correct” solution, in the sense that the archipelago override sequence hindcast by tomotectonics in Section 4.4 will terminate with the spatial configuration of today’s Cordilleran accreted terranes. The slab/arc associations must also satisfy the geologically known timing constraints during the arc accretion sequence. In figure 7, the current and former instances of arcs are grouped into superterranes and linked by their unchanging colors over time: Farallon arcs and slabs in green, Insular (INS) & Guerrero (GUE) microcontinents in orange; Intermontane (IMS) microcontinent in purple; and Central Alaskan arcs in red. Our slab/arc matches are justified in sections 5.1 and 5.2.

5.1 Northern and southern Farallon arcs (eastward subduction)

Upper-mantle FN slab must be matched with the Cenozoic, still active Cascades arc (du Bray et al, 2014; Tepper and Clark, 2024; though a continuous arc axis is only apparent since ~40 Ma, see Fig. 1 of Glazner, 2022). This match is straightforward in terms of latitudinal extent, timing, polarity, and continental character.

It is less clear which arc terranes to associate with older northern Farallon subduction, i.e., with the voluminous lower-mantle CR slab, schematically drawn as light green patch in fig. 7 in its stationary, slab-wall position and strike. Expected to be oceanic in character and accreted inboard of today’s Cascades arc, CR arc may well be best preserved in the subsurface beneath Vancouver Island (Clowes et al., 1987) as the downdip extent of the Pacific Rim terrane (“PR” in fig. 7; Sigloch & Mihalynuk 2013, 2017).

In addition, parts of CR arc may have been entrained and transported north with BajaBC and the successor transform regime that continues to today (e.g., Baranov-Leech River hypothesis of Cowan, 2003; Garver and Davidson, 2015). That such a big and old slab has only fragmentary arc relics illustrates some practical challenges in making slab/arc matches. However, this is equally true for any accounting of pre-Cascades subduction in the Pacific Northwest from geology or plate tectonics alone. FAR-PAC isochrons record Farallon spreading towards the Pacific Northwest since 180 Ma, irrespective of mantle evidence. If the pre-Cascades arc were postulated to have grown on the margin, the problem of the “missing” arc would be aggravated because such an arc should not be displaced as easily as the intra-oceanic CR arc inferred by tomotectonics.

Another straightforward match is the association of FS slab with the arc that built the Sierra Nevada Batholith (SNB, essentially ~120-80 Ma, Paterson and Ducea, 2015). FS slab fits the timing, subduction polarity and continental nature of the SNB arc. Fig. 7 shows this arc in green, originating at the eastern tip of FS slab, in the inner corner between MEZ and ANG slab walls. The dashed, retreating trench lines

schematically represent the subsequent, southwestward migration of this arc with the NAM margin while the FS slab grows below it.

In the southern U.S. sector, no clear arc axis younger than the SNB is observed, consistent with the slab-free region southwest of FS slab. Post-SNB volcanism and magmatism in the region are spatially diffuse instead of linearly aligned, not of typical arc chemistry (see Glazner, 2022).

For completeness, the Pacific plate subducts northward beneath southern Alaska today. This subduction zone has been building the upper-mantle Aleutians slab (Gorbatov, et al., 2000; van der Meer et al., 2018), associated with the Aleutians arc since at least 46 Ma (Jicha and Kay, 2018). This obvious match is mentioned here because Baja-BC shuffling events transported southern Alaska terranes (Insular Superterrane) to its present resting place by ~50 Ma (e.g. Kent and Irving, 2010), just before Aleutians subduction initiated and the Aleutian arc started to grow on and outboard of those newly arrived terranes (northward translation of outermost INS is still happening due to coupling across the active dextral transform margin). Earlier Kula subduction events in that region (presumably matched with KI slab in figs. 5 and 3, (Sigloch & Mihalynuk 2017) do not directly pertain to the present study.

5.2 Arcs associated with Mezcalera/Angayucham westward subduction

Section 5.1 has matched all eastward (Farallon) arcs inferred by tomotectonics with actually observed geological arcs. The tomotectonically inferred arcs (i.e., slabs) remaining to be matched are MEZ and ANG. Conversely, five geological arc systems of Cretaceous and Jurassic age remain to be matched to slabs (Fig. 7), from north to south: the Cretaceous arcs of Central Alaska (Koyukuk); the arcs on the Insular Superterrane (INS: Wrangellia, Alexander and Peninsular terranes); arcs on the Intermontane Superterrane (IMS: Stikine and Quesnel); the Native Triassic-Jurassic arc in the southwestern U.S.; and the Cretaceous arc on the Guerrero Superterrane in Mexico.

At times preceding the main SNB flare-up 125-85 Ma (Paterson and Ducea, 2015), arc volcanism was built on Insular Superterrane (INS) (205-165 Ma, younging eastward; Canil and Morris, 2024). According to paleomagnetic evidence (Kent & Irving 2010), INS lay at latitudes of the southern U.S. and northern Mexico when its Jurassic arc was active, but now occupies an outboard position along the margins of B.C. and southern Alaska – hence the name “Baja-BC” (Irving, 1985) for the margin-parallel shuffling that achieved the displacement between 90 and 50 Ma.

Construction of the “Native Triassic-Jurassic arc” (256 Ma (latest Permian) to 175 Ma) on the cratonic margin of the southwestern U.S. was followed (~170 Ma) by a period of transpression and formation of Middle Jurassic ophiolites (Saleeby and Dunne, 2015). Most workers refer to the Jurassic magmatic rocks as parts of an extensional continental arc (Tosdal and Wooden, 2015; Saleeby and Dunne, 2015; Busby and Centeno-García, 2022), that transitions southward to the opening Gulf of Mexico. What proportion of these arc-type volcanic and plutonic rocks (which typically display extensive interaction with the Proterozoic crust) are true arc versus decompression melts related to extension, is an open question. Zircon geochemistry shows elevated Th/U ratios of Sierra-Nevada-derived Jurassic detrital zircons of southeast California (180-160 Ma, Barth et al., 2013) are atypical of arc zircons from both older, Triassic, and younger, Cretaceous, Sierra Nevadan magmatic rocks, and may be from asthenospheric sources (Tosdal and Wooden, 2015).

Intermontane Superterrane (IMS) in British Columbia, located inboard of INS, hosted another long chain of Triassic-Jurassic arcs (Stikine & Quesnel) that went extinct and were accreted by ~174 Ma (Mihalynuk

et al., 2004). Before accretion, IMS presumably formed the offshore, northwestward extension of the Native arc in western USA, judging by their geographic and geological relationship [REF] and their almost simultaneous demise or change to extensional regime between ~170 and ~180 Ma (Barth et al., 2013; Tosdal and Wooden, 2015, see above).

The slab wall of northern MEZ lies in spatial and temporal continuity with FS slab, which was built ~130-80 Ma (fig. 1). Hence the Native arc would be too ancient for a match to MEZ slab, and as a margin-hugging arc it must necessarily have been eastward-subducting, whereas MEZ slab accommodated westward subduction (section 4.3, 4.4). IMS arcs cannot be directly paired with MEZ for the same timing reasons: they do not nearly reach to 130 Ma.

The geologic arc to associate with MEZ slab can therefore only be the Jura-Cretaceous arc on INS. This is plausible because INS is not part of stable North America but rather an accreted microcontinent. Hence westward subduction beneath INS is possible *a priori*, but paleo-seafloor east of INS would need to be demonstrated, as a match for the tomotectonically inferred Mezcalera Ocean.

Towards the east, INS is indeed separated from IMS by a belt of “collapsed basins” of oceanic character. Sigloch & Mihalynuk (2013, 2017) made detailed geological arguments why these collapsed basins are suitable to represent the suture of the tomotectonically inferred Mezcalera-Angayucham Ocean (light blue in fig. 7). A rough dozen of collapsed basins are shown on their present-day positions (also light blue in fig. 7), and named in the legend. They have the correct ages (sufficiently young from detrital zircon dating), spatial extent (spanning the length of the NAM margin) and character (mantle slivers outcropping in half of the basins) in order to represent the suture of the Mezcalera-Angayucham Ocean that closed west of MEZ slab by westward subduction.

MEZ slab wall runs south to Mexican latitudes. There are suitable geological matches in the Cretaceous arc on Guerrero Superterrane, a southern correlate of INS Superterrane (fig. 7). The collapsed basin representing the Mezcalera ocean (and its suture) to the west of Guerrero is the Arperos basin, adopting an interpretation of Tardy et al. (1992) and Dickinson and Lawton (2001). An additional Mexican arc, the Early Cretaceous Alisitos arc that preceded Farallon subduction (accreted outboard of Guerrero arc) is considered out of spatial scope but is matched to slab by Clennett et al. (2020).

The Cretaceous arcs of Central Alaska are a straightforward match with ANG slab wall. Figure 1 shows how NAM underrode ANG slab very slowly over Cretaceous times and into the Cenozoic – a prolonged, oblique collision that would have slowly plucked the originally linear, >3,000 km long arc off its slab and crumpled its slivers into the tightly folded oroclines seen in figure 7 (in red). The northerly latitude of ANG slab ensures that Central Alaska accretes north of all Farallon and MEZ arcs, as observed. This huge slab provides a satisfying placement for Central Alaskan terranes that have been difficult to place or to relate to more southerly events in reconstructions based purely on geology (e.g. Patton and Box, 1989) or purely on plate reconstructions (e.g., Seton et al. 2012).

With this, all arcs back to ~170 Ma are matched to slabs, and all slabs in figure 1 are matched to arcs. The two oldest candidate arcs, Native arc and IMS (Stikine, Quesnel), remain unmatched to slab. This is unsurprising in light of our tomotectonic inference that the Archipelago to 1800 km depth records events since Pangaean breakup and Atlantic spreading. The ~170 Ma extinction of a long, linear chain of Native/Intermontane arcs, and its sudden replacement by the even more vast MEZ and ANG arcs, must be a consequence of hemispheric reconfiguration of the time. Sigloch & Mihalynuk (2017, 2020) speculatively matched slab below the Atlantic to the Native/IMS arc, albeit not directly below the 170-Ma position of NAM in fig. 1. The uncertainties of absolute paleo-positioning multiply into Jurassic times,

with neither surviving seafloor nor hotspot tracks available, and lingering questions about True Polar Wander (Fu & Kent, 2018).

5.3 Archipelago override sequence replayed with arc terranes

We replay the archipelago override sequence of Section 4.4 with the matched geologic arc terranes. The most relevant figures are figures 7, 6 and 5. Events are narrated with an emphasis on slab pull as the driving force. This is justified by the observation that 90% of present-day plate motions can be explained by trench configurations: plates mainly seem to move because they are pulled perpendicularly into subduction zones where dense slab is sinking into the mantle (Forsyth & Uyeda, 1975).

In the proto-Pacific basin, a vast grouping of intra-oceanic arcs starts up relatively simultaneously between 205-180 Ma. This new Archipelago sits >1,000 km west of NAM and consists of arcs that built the Insular-Guerrero Superterrane, a Mesozoic-Paleozoic microcontinent; and future Central Alaskan arcs, striking NW-SE along a >3,000 km trench. Further to the west, the new Farallon arc parallels the strike of the Alaskan (ANG) arcs over ~2,000 km length, sitting ~1,500 km south of them. On and close to the NAM margin, a long chain of older arcs is shutting down (Native & IMS), are overprinted, or transition southward into extensional volcanic fields (e.g. Saleeby and Dunne, 2015; Tosdal and Wooden, 2015; Busby and Centeno-García, 2022). NAM is exposed to westward pull because the seafloor west of it, which forms part of the NAM plate, is now subducting westward beneath the INS-GUE and Central Alaskan arcs (MEZ & ANG slabs). A rift zone between eastern NAM and west Africa transitions to full-blown westward drift by ~170 Ma, opening the Central Atlantic along a spreading ridge that is parallel to the INS-GUE trench.

Thus North America breaks away from Pangaea and is pulled into the Archipelago, with INS-GUE trench consuming the seafloor immediately west of NAM, the Mezcalera Ocean. Around ~150 Ma, NAM first collides with northern INS at U.S. latitudes: at the easternmost point of the Archipelago, the Mezcalera Ocean has closed and collapsed into a suture. This continent-microcontinent collision deforms the margin locally (Nevadan orogeny), and the accreted (obducted) INS loads the continental margin, which develops topography in B.C. that sheds sediments inland (Passage Beds of B.C. ~155 Ma. The collided segment of INS arc becomes extinct (Sierra Nevada segment).

NAM continues to be pulled into the Archipelago by the still-subducting segments of the Mezcalera and Angayucham Oceans, south and north of the collided segment. As NAM rides into the interior of the Archipelago, the seafloor sitting there is forced to subduct under the continental margin, i.e., eastward. Therefore a new arc is constructed above the lithosphere now subducting eastward beneath the continental margin. This is the SNB arc, which intrudes and overprints two older arcs: the accreted, extinct INS arc and the Native Triassic-Jurassic arc (extinct since 170 Ma) on stable NAM. The evolution of the override sequence and the three juxtaposed arcs is shown in fig. 8a.

NAM continues to be pulled west by the southern MEZ and by ANG subduction zones. They are trenches on a suicide mission: the continent collides with wider and wider (in latitude) swaths of INS-GUE arc segments, which go extinct and are replaced by eastward SNB arc. From ~110 Ma, NAM also collides with future Central Alaskan arcs along ANG slab (fig. 1). At latitudes of the CR (Fig. 1) ANG trench segments are not polarity-flipped due to the intervening Orcas micro-plate (Orcas MP), which can slide out of the way rather than subduct.

Progressive accretion of arc segments intensifies the deformation of the margin, and widens it in latitude into the Sevier and Canadian Rocky Mountain orogenies. Fig. 8b shows this widening and deepening of margin deformation over time, radiating out from the Nevadan orogeny (in red).

The progressive closure of the Mezcalera Ocean between INS and NAM forms the collapsed basins of fig. 7, predicted by tomotectonics (fig. 1) to have closed from ~150 Ma (in the U.S.) to ~100 Ma (in MX), as INS diachronously collided with NAM or with IMS (where IMS was pre-accreted to NAM).

Around 100 Ma, the Insular-Guerrero arc was extinct even in Mexico – the end of westward subduction at MX, US and southern BC latitudes. The Yukon margin and northern BC continued to be pulled into the Koyukuk arc. Farallon eastward subduction now reigned in the south: the SNB arc on the margin (FS slab) had expanded south along the Mexican margin to form the Peninsular arc (Dickinson and Lawton, 2001). The northern Farallon arc (Pacific Rim terrane, and more) remained offshore, but by 90 Ma probably felt the approach of the NAM margin, which had reached the Orcas microplate, which became substrate for both northern Farallon arc and the Koyukuk arc construction.

Around 80 Ma, the SNB arc on the margin suddenly shuts down (Big Break), probably related to the complications to its north and southern collision of the Hess-Shatsky Rise conjugate plateau (Livaccari et al., 1981; Humphreys, 2009; Humphreys et al., 2015). The sudden demise of this long, margin-hugging trench decouple the Sierra Nevada-Peninsular segment of the margin, specifically the accreted INS and IMS. Farallon plate transitions into transform motion (transpression) relative to NAM, and the transform boundary runs inside the soft continental lithosphere. Thus slivered-off parts of accreted INS and IMS (“Baja-BC”) can move north rapidly, quasi as parts of the Farallon plate. Since the northern Farallon arc still sits offshore, Baja-BC can move north relatively unimpeded and *inboard* of the northern Farallon arc, assisted by the small, moveable Orcas microplate (as spelled out in section 6.2).

This transform corridor stays open for some tens of m.y. (recorded by disruption and retreat of upper CR slab), until by ~50 Ma the Orcas plate has gone, the northern Farallon trench has obliquely accreted to the Pacific Northwest margin, and established a new arc on the margin (Cascades arc). This margin-hugging new Farallon arc acts like a roadblock that ends the free passage of Baja-BC terranes.

The transform margin along the Sierra Nevada sector (San Andreas) continues to present, still slivering off continental fragments and transporting them north (Baja California, Salinian block, Transverse Ranges...) but only until they reach the impasse of the Juan de Fuca (northern Farallon) plate and its Cascades arc.

In the far north, the Koyukuk arcs have been slowly crumpling against the NAM margin (fig. 9b, at 85 Ma), when Baja-BC starts arriving from the south. Baja-BC gets wedged against the backstop of the Koyukuk arcs. As the Orcas microplate gets squeezed away or subducts, the INS and Central Alaskan arcs are compressed into the big terrane agglomerate that is Alaska (fig. 9b).

Once the Koyukuk arc is completely extinct (ANG slab largely overridden by 50 Ma), the margin becomes a transform. It remains a transform boundary to the present-day, still carrying parts of INS northward, albeit more slowly, at ~41 mm/yr (Leonard, et al., 2007).

6. Discussion

We first discuss the range of collision styles encountered (mainly ~150 to 90 Ma), followed by the discussion of margin-parallel translations (“Baja-BC”, since ~90 to 50 Ma).

6.1 Double-sided subduction caused and shaped all collisions since 150 Ma

All arc collisions in the Archipelago were shaped by double-sided subduction. Double-sided subduction, from roughly the east and the west, are arguably the defining feature of the Archipelago from its inception (fig. 6a). When the three major intra-oceanic arcs of MEZ, ANG and Farallon (CR) spring up all around the same time (1800-2000 km depth, corresponding to the early Jurassic), they reconfigure the eastern proto-Pacific from scratch. The chosen arrangement is that of double-sided subduction – Farallon (CR) subduction directly facing off with ANG subduction (parallel trenches, with the Orcas microplate as a passive spacer in between), and MEZ subduction in a similar role as ANG, although striking more obliquely to CR (fig. 6a). The “function” of this geometry is to permit two large ocean domains (Farallon Ocean and Mezcalera-Angayucham Ocean) to subduct simultaneously, in a configuration that can remain stable over long time scales. Presumably this is the most efficient mode of cooling the mantle, hence preferred by the earth. A very close analogue currently exists in the southwest Pacific, as detailed by Sigloch & Mihalynuk (2017). The Pacific Ocean and the Indian (formerly Tethys) Ocean subduct into this region from opposite sides without much disruption. The interior of the archipelago – the region circumscribed by the Sunda arc, Papua-New Guinea, the Coral Sea arcs, and the Izu-Bonin and Mariana arcs – is complex in detail, with shifting configurations of minor trenches. Yet the basic functioning, of letting two big oceans subduct from the exterior, is robust – slab walls are observed below the bounding trenches (e.g., Hosseini et al., 2020).

However, the pull exerted by an archipelago also pulls in large continents, like present-day Australia, or Cordilleran North America. When the continent collides with segments of the arcs, yet keeps getting pulled in by adjacent, still-active arc segments, the archipelago slowly puts itself out of business. For the Cordilleran archipelago, these self-defeating dynamics led to its complete demise.

6.1.1 Southern U.S. and Mexico: heads-on collision with subduction flip

In the first stage of Archipelago collisions, North America collided “only” with an eastward-protruding part of MEZ arc, while continuing to be pulled west by more southerly segments of MEZ and by all of ANG. It is crucial to not think of this collision merely in 2-D as cartooned in fig. 8a: in and out of the plane (at Mexico and B.C. latitudes), westward subduction kept pulling the NAM plate westward even after this pull had ceased on the U.S. ~150 Ma. The override of MEZ led to a gradual, orderly polarity flip along the collided segments, diachronous from the U.S. to Mexico. Intra-archipelago “southern Farallon” lithosphere (FS) was forced beneath the invading continental margin (first in the U.S., then also Mexico), in the sequence cartooned by figure 8a. A close analogue is the trench flip underway at the northern margin of Australia (Papua-New Guinea), which has breached the previously uninterrupted chains of Sunda and Coral Sea arcs, and keeps getting pulled further northward by the surviving segments of those two arcs (Sigloch & Mihalynuk 2017).

The NAM-MEZ collision was thus succeeded by a sizable margin-hugging arc (FS slab) that built the SNB & Peninsular batholiths over ~40 m.y. (120-80 Ma). This arc shut down suddenly in the Big Break ~80 Ma, according to tomotectonics (fig. 1). It is difficult to isolate specific causes in such an interconnected plate-mantle system, but ultimately the SNB arc probably died because the motivating force, of pull into the Archipelago, gradually ceased due to MEZ-ANG override, perhaps aided by arrival

of the Hess-Shatsky plateau conjugate, which was difficult to subduct (Livaccari et al. 1981). The paleo-margins in fig. 1 progressed westward more and more slowly over time.

6.1.2 Pacific Northwest, B.C., Alaska and “Baja-BC”: collisions “shielded” by double-sided subduction.

In the late stage of arc collisions, NAM overrode the opposing ANG and CR trenches simultaneously and very obliquely (since ~100 Ma). Subduction could not flip in the course of ANG override, essentially because the opposing polarity (eastward Farallon/CR) had already been present since the beginnings. Only the Orcas microplate might have been forced under NAM in a short-lived polarity flip, but in practice it seems to have been squeezed out toward the west. The ability to laterally translate this microplate quickly was likely the key to producing the rapid Baja-BC shuffle while Baja-BC was coupled to this microplate (fig. 9 and section 6.2.). In this configuration, double-sided subduction, the defining feature of the Orcas microplate, facilitated two other collision styles: the slow crumpling against NAM of the Koyukuk arcs (which were welded into the microplate), and the northward sprint and squeeze of Baja-BC against the Koyukuk arcs, which assembled Alaska by ~50 Ma (fig. 9b). Both these styles were possible because the pre-existing CR trench of opposing polarity shielded the NAM margin and the ANG arcs from the compression of a margin-hugging trench, which would have resulted from a polarity flip in the style of the SNB arc.

6.1.2 Tomotectonic hypothesis testing on the three Sierra Nevada arcs

The field geologic record of the arc extinction / trench flip sequence is complex, because (at least) two arcs are produced in the same place (figure 8a). For MEZ, westward subduction ahead of the first-colliding margin segment (U.S. Sierra Nevada segment) was of decent duration, from MEZ/INS arc inception ~200 Ma(?) to first collision ~150 Ma. However, the geologic record of this INS arc is obscured by a later, overprinting arc, the Sierra Nevada Batholith arc (figure 8a, bottom). This overprinting is not an unlucky coincidence but an inevitable consequence of the arc collision / trench flip sequence. It is systematically predictable here and elsewhere (e.g., Papua-New Guinea or Taiwan).

Tomotectonics can contribute to geologic field studies the guiding hypothesis that a suture basin should be present within the arc zone (here it is found in the Calaveras mélangé belt, and collapsed Mariposa basin, fig. 7), and that westward-subduction (INS) plutons should be found only *outboard* of this Mezcalera Ocean suture (whereas the later SNB arc may produce plutons inboard and outboard). Testing this hypothesis requires precise timing constraints, where the biggest challenge is to reliably distinguish plutons that are strictly of arc character (i.e., caused by down-going Mezcalera plate and thus really dating the westward subduction episode), from plutons that are due to post-arc flare-up or to remelting of older arc plutons. If the latter types are confused for the former, the dating constraints and hypothesis testing go awry.

What might be an unlucky coincidence in the Sierra Nevada case is the existence of a third, older arc (Native arc on the margin, extinct by 170 Ma), which was nearing extinction, but was still active when INS arc started up. Prior to ~170 Ma, those two arcs were >1,000 km apart, but now they are separated only by the narrow suture. As an eastward-subducting arc, Native arc is predicted to intrude only on the *inboard* side of the suture. Hence the suture must be well mapped and understood, in order not to confound Native arc plutons for INS plutons. For example, erroneously attributing a Native arc pluton that is located inboard of the suture to INS arc, would lead to the erroneous rejection of the hypothesis that an ocean was separating NAM from INS before ~150 Ma.

Unless the predicted suture is systematically kept in mind, the westward subduction episode may escape notice entirely: inboard of the suture, Native arc is attributed plutons as late as 170 Ma (Dickinson, 2008), and the flipped SNB arc might have produced its first plutons east (and west) of the suture very soon after subduction flip ~ 150 Ma. A pluton hiatus from 170 to ~ 150 Ma east of the Mariposa basin would not appear noteworthy if not with this specific hypothesis in mind. Even then it will be challenging to robustly resolve a 20 m.y. time window of arc hiatus (by reliably rejecting all non-arc volcanism from consideration).

We finish with the caution that the north-south ordering of MEZ suture basins in fig. 7 is almost certainly not the same as their original north-south ordering, which has been scrambled by Baja-BC shuffling. This needs to be kept in mind when predicting suturing dates, and hence plutons on either side. To our present understanding, the Sierra Nevada segment should have the oldest MEZ suture (~ 155 Ma), the Guerrero segment the youngest suture (~ 110 Ma), and neither segment has been transported north to a significant degree. Locations that sutured between these original latitudinal limits of INS accretion are predicted intermediate suturing dates, but these basins have since been transported to British Columbia and southern Alaska. Hence we cannot naively predict that northern basins should have older sutures than southern ones, even though that is what the override sequence of MEZ slab in fig. 1 would suggest. Baja-BC events must be restored before interpreting the older accretion record.

6.2 Tomotectonics infers BajaBC displacements, independent of paleomagnetism

“BajaBC” is a long-standing hypothesis developed to explain paleomagnetic measurements on Cordilleran terrestrial rocks, reproduced many times (Kent & Irving 2010), which indicate that Insular microcontinent and western parts of Intermontane microcontinent (Stikinia) originally accreted far south of their current locations, relative to NAM. Southern INS, now located in southern British Columbia, originally occupied Baja Californian (Mexican) latitudes (Irving 1985, Kent & Irving 2019). Alaskan parts of INS should accordingly have accreted at U.S. latitudes. The northward shuffle of 1500-2000 km happened between 90 Ma and ~ 50 Ma because rocks magnetized before 90 Ma show the full latitudinal offset, and rocks magnetized after 50 Ma show no significant offset to their present-day location.

INS constitutes the largest part of Baja-BC. Tomotectonics infers that INS indeed must have undergone large-scale northward displacement since its accretion, in an argument completely independent of rock magnetism. Figure 1 hindcasts that first accretion of INS to NAM at ~ 150 Ma occurred at U.S. latitudes (California and/or Pacific Northwest). This first collision involved northeastern promontory of MEZ slab, hence northern INS arc. Today, northernmost INS arc (Peninsular/Alexander terranes) is not abutting the U.S. but the southern Alaskan margin. Thus tomotectonics infers that since its accretion, northern INS must have moved north relative to stable NAM, from U.S. latitudes to Alaskan latitudes. This amount of displacement is consistent with paleomagnetic data mainly from *southern* INS (southern B.C., Washington state), which infer an original location at Mexican or southern U.S. latitudes. Tomotectonics therefore provides remarkably straightforward support for paleomagnetic measurements that have still not gained widespread acceptance within the geologic community.

Figure 9a shows the trajectories over time of the half dozen most robust paleomagnetic data sets that gave rise to the Baja-BC hypothesis. Data from many more sites support the timing of the northward sprint, but are less robust on the amount of displacement. The blue/green trajectories follow the paleomag sites back in time and space to where and when they were magnetized: Carmacks at 70 Ma, Churn Creek/Mount Tatlow at 95 Ma, 103 Ma for Spences Bridge, etc. (Enkin, 2006). All positions are given in absolute coordinates relative to the lower mantle. The Baja-BC sites are implemented to move

northward rapidly between 70 Ma and 50 Ma. (This was a choice given other tomotectonic constraints. Any time period between 90 Ma and 50 Ma is admissible.)

The yellow line is our speculation for where the main Baja-BC transform fault ran. It is necessary to commit to a location when building a quantitative model like Clennett et al. (2020). We run the main Baja-BC shear inboard of all displaced sites of fig. 9a, but no more inboard than necessary (a conservative solution), and in locations that can plausibly hide a major fault. Mainly we run the fault through Intermontane terranes now located in B.C. and through presumed, left-behind IMS correlatives in the U.S. (in or west of the Blue Mountains)(Mihalynuk & Diakow 2020, Tikoff et al. 2023).

In B.C., we speculate that the fault runs through the Cache Creek accretionary complex, sliding Stikinia past Quesnellia (as in fig. 9b at 85 Ma). Displacement of Quesnellia is inferred to have been much less than Stikinia; however, paleomagnetic data on layered volcanic rocks atop Quesnellia that are not compromised by resetting and pass all confidence tests, have yet to be obtained. Hence we position the main Baja-BC shear zone conservatively between Quesnellia and Stikinia; the intensely imbricated Cache Creek terrane which separates them could well hide this shear zone. In the Pacific Northwest U.S., its offset must be distributed somewhere between the dashed and the non-dashed line.

In California, we run the fault slightly outboard of the NAM-INS suture (identified with the Calaveras mélangé belt & Mariposa collapsed basin in the Sierra Nevada; figure 7). The rationale is that not much of INS should be left in California if it is now found mainly in B.C. In practice, this means that we run the fault under the Central Valley, inspired by Wright and Wyld (2007), but we continue it *inboard* of the Klamaths, in order to implement ~1000 km northward translation of the Klamaths (Housen and Dorsey, 2005), past the stationary Sierra Nevada), which is recorded by Ochoco basin strata that straddle the Klamath block (Housen, 2018). At the large scales considered in this study, the uncertainties about the exact location of the fault(s) do not change any conclusions.

In the tomotectonic accounting for Baja-BC, an important role is played by the space between the two ancient, stationary and opposing slab walls ANG and CR. This space was necessarily occupied by a (micro-)plate, named “Orcas” by Sigloch & Mihalynuk (2013), into which the ANG and CR arcs were welded since the inception of the Archipelago. There they presumably sat unperturbed until NAM overrode this double-sided trench pair obliquely between ~100-50 Ma. Figure 9b shows the Clennett (2020) reconstruction at 85 Ma. Baja-BC displacement has started, and Stikinia/INS are being carried past Quesnel, carried by the main shear fault in the Cache Creek complex (yellow). Crucially, Baja-BC has effectively become a part of the Orcas microplate – the yellow shear fault forms Orcas’ eastern plate boundary against NAM. This small plate can presumably move and subduct very fast, carrying Baja-BC along (the northward “sprint”). Orcas is squeezed from the east by NAM and probably subducts westward. The Central Alaskan arcs (ANG) have always been welded into the Orcas micro-plate, and fig. 9b details how this facilitates the assembly of All-Alaska on and by the Orcas plate.

Orcas microplate may have quickly subducted into the small upper-mantle slab that strikes east-west under southern Saskatchewan, Alberta and B.C. (dark blue in fig. 3a). This slab is not part of the sloping continuity of the northern Farallon group, but rather seems to rest on top of it. Its location in fig. 9b is marked by the gray oval and two “??”, a very plausible place for Orcas MP to have been squeezed into.

7. Conclusions and outlook

We have explained the tomotectonic method on a fully worked example for NAM. The method is based on a very simple, predictive, falsifiable null hypothesis, and a separation of geophysical (slab and plate tectonic) observations for making predictions, from geological observations for testing the predictions. The link between tomotectonics and geology is made by volcanic arcs in subduction zones.

Since breaking away from Pangaea in early Jurassic times, North America has overridden a vast archipelago of intra-oceanic subduction zones and their arc terranes. This is supported by very robust evidence in the mantle and at the surface. An archipelago is an oceanic area bounded by trenches that are oriented to pull in seafloor from two opposite sides: a large-scale zone of plate convergence. All arc and microcontinent collisions of Cordilleran North America since ~150 Ma have been shaped by this double-sided nature of subduction. Different collision and deformation styles have occurred depending on the spacing of the two opposing trenches, and the angle at which North America collided with their arc terranes.

The accretion of Insular Superterrane, including the Sierra Nevada arc succession and orogeny was a case of subduction flip within the spacious interior of the archipelago. Oroclinal collapse of the Central Alaskan arcs against the continental margin by westward subduction was possible in the “wind shadow” of a nearby, opposite-facing Farallon trench. The northward sprint of Baja-BC and its collapse against Central Alaska was a product of the same environment of closely spaced, opposing trenches.

Tomotectonics infers the large-scale northward displacement of Insular Superterrane (relative to stable North America) since it accreted. This inference is completely independent of the paleomagnetic argument for Baja-BC, and supportive of it.

A good understanding of these large-scale margin-parallel displacements between 90-50 MA is crucial for the correct interpretation of the older accretions that pre-date Baja-BC, including the evidence for westward subduction. Slabs can unscramble this record because they have stayed in their absolute paleo-positions, while surface elements have been much more mobile.

The tomotectonic null hypothesis, of subducted lithosphere sinking basically vertically once it has entered its trench, is holding up well so far. With very few degrees of freedom, it capably predicts the known regional tectonic regimes (subduction, compression, transform) and their changes along various sectors of the NAM west coast from ~170 Ma to today. An area where geologists could make very useful contributions to tomotectonic hypothesis testing is the precise diagnosis of arc versus non-arc magmatism.

8. References

- Atwater, T., 1970, Implications of plate tectonics for the Cenozoic tectonic evolution of western North America: Geological Society of America Bulletin, v. 81, p. 3513–3536.
- Atwater, T., 1989, Plate tectonic history of the Northeast Pacific and western North America, in Winterer, E.L., Hussong, D.M., and Decker, R.W. eds., The eastern Pacific Ocean and Hawaii, Geological Society of America, Decade of North American Geology, v. N, p. 21–72.
- Barth, A.P., Wooden, J.L., Jacobson, C.E. and Economos, R.C., 2013, Detrital zircon as a proxy for tracking the magmatic arc system: The California arc example. *Geology*, 41(2), p. 223-226.

- Bunge, H.P. and Grand, S.P., 2000, Mesozoic plate-motion history below the northeast Pacific Ocean from seismic images of the subducted Farallon slab. *Nature*, 405(6784), p.337-340.
- Busby, C.J. and Centeno-García, E., 2022, The “Nazas Arc” is a continental rift province: implications for Mesozoic tectonic reconstructions of the southwest Cordillera, US and Mexico. *Geosphere*, 18(2), p. 647-669.
- Busby, R.W. and Aderhold, K., 2020, The Alaska transportable array: As built. *Seismological Research Letters*, 91(6), pp.3017-3027.
- Canil, D. and Morris, R.A., 2024, Continentalization of an intraoceanic arc as exemplified by the Jurassic Bonanza arc of Vancouver Island, Canada. *Bulletin*, 136(1-2), p. 880-892.
- Cerpa, N.G., Sigloch, K., Garel, F., Heuret, A., Davies, D.R. and Mihalynuk, M.G., 2022, The effect of a weak asthenospheric layer on surface kinematics, subduction dynamics and slab morphology in the lower mantle. *Journal of Geophysical Research: Solid Earth*, 127(8), p.e2022JB024494.
- Chapman, A.D., Saleeby, J.B., Wood, D.J., Piasecki, A., Kidder, S., Ducea, M.N. and Farley, K.A., 2012, Late Cretaceous gravitational collapse of the southern Sierra Nevada batholith, California. *Geosphere*, 8(2), p. 314-341.
- Clennett, E.J., Sigloch, K., Mihalynuk, M.G., Seton, M., Henderson, M.A., Hosseini, K., Mohammadzahari, A., Johnston, S.T. and Müller, R.D., 2020, A quantitative tomotectonic plate reconstruction of western North America and the eastern Pacific basin. *Geochemistry, Geophysics, Geosystems*, 21(8), p.e2020GC009117.
- Clowes, R.M., Brandon, M.T., Green, A.G., Yorath, C.J., Brown, A.S., Kanasewich, E.R., and Spencer, C., 1987, LITHOPROBE-southern Vancouver Island: Cenozoic subduction complex imaged by deep seismic reflections: *Canadian Journal of Earth Sciences*, v. 24, p. 31–51.
- Cowan, D.S., 2003, Revisiting the Baranof-Leech River hypothesis for early Tertiary coastwise transport of the Chugach-Prince William Terrane: *Earth and Planetary Science Letters*, v. 213, p. 463–475, doi: 10.1016/s0012-821x(03)00300-5.
- Cowan, D.S., Brandon, M.T. and Garver, J.I., 1997, Geological tests of hypotheses for large coastwise displacements; a critique illustrated by the Baja British Columbia controversy. *American Journal of Science*, 297(2), p. 117-173.
- Dickinson, W.R., 2008, Accretionary Mesozoic-Cenozoic expansion of the Cordilleran continental margin in California and adjacent Oregon: *Geosphere*, v. 4, p. 329–353, doi: 10.1130/GES00105.1.
- Dickinson, W.R., and Lawton, T.F., 2001, Carboniferous to Cretaceous assembly and fragmentation of Mexico: *Geological Society of America Bulletin*, v. 113, p. 1142–1160.
- du Bray, E.A., John, D.A. and Cousens, B.L., 2014, Petrologic, tectonic, and metallogenic evolution of the southern segment of the ancestral Cascades magmatic arc, California and Nevada. *Geosphere*, 10(1), p. 1-39.
- Dumitru, T.A., Wakabayashi, J., Wright, J.E., and Wooden, J.L., 2010, Early Cretaceous transition from nonaccretionary behavior to strongly accretionary behavior within the Franciscan subduction complex: *Tectonics*, v. 29, <http://onlinelibrary.wiley.com/doi/10.1029/2009TC002542/full>.
- Earth Model Collaboration, 2024, A repository of Earth models providing the NSF SAGE and GAGE research community model preview visualization tools, facilities to extract model data/metadata, and access to the contributed processing software. URL: Earth Model Collaboration / EarthScope Consortium | Observable (observablehq.com) [accessed July, 2024].

- Engebretson, D.C., Cox, A., and Gordon, R.G., 1985, Relative motions between oceanic and continental plates in the Pacific basin: Geological Society of America Special Paper 206, p. 1–60.
- Enkin, R.J., 2006, Paleomagnetism and the case for Baja British Columbia: Paleogeography of the North American Cordillera, in Haggart, J. Enkin, R.J. and Monger, J.W.H., eds., Paleogeography of the North American Cordillera, Evidence For and Against Large-Scale Displacements: Geological Association of Canada Special Paper 46, p. 233–253.
- Forsyth, D. and Uyeda, S., 1975, On the relative importance of the driving forces of plate motion. *Geophysical Journal International*, 43(1), p. 163-200.
- Fu, R.R. and Kent, D.V., 2018, Anomalous Late Jurassic motion of the Pacific Plate with implications for true polar wander. *Earth and Planetary Science Letters*, 490, p. 20-30.
- Garver, J.I. and Davidson, C.M., 2015, Southwestern Laurentian zircons in upper Cretaceous flysch of the Chugach-Prince William terrane in Alaska. *American Journal of Science*, 315(6), p. 537-556.
- Gorbatov, A., Widiyantoro, S., Fukao, Y. and Gordeev, E., 2000, Signature of remnant slabs in the North Pacific from P-wave tomography. *Geophysical Journal International*, 142(1), p. 27-36.
- Hildebrand, R.S., 2009, Did westward subduction cause Cretaceous-Tertiary orogeny in the North American Cordillera? v. 457. Geological Society of America.
- Hildebrand, R.S., 2013, Mesozoic assembly of the North American cordillera v. 495. Geological society of America.
- Hosseini, K., and Sigloch, K., 2015, Multifrequency measurements of core-diffracted P waves (Pdiff) for global waveform tomography: *Geophysical Journal International*, v. 203, p. 506–521.
- Hosseini, K., Matthews, K.J., Sigloch, K., Shephard, G.E., Domeier, M. and Tsekhmistrenko, M., 2018, SubMachine: Web-based tools for exploring seismic tomography and other models of Earth's deep interior. *Geochemistry, Geophysics, Geosystems*, 19(5), pp.1464-1483.
- Hosseini, K., Sigloch, K., Tsekhmistrenko, M., Zaheri, A., Nissen-Meyer, T. and Igel, H., 2020, Global mantle structure from multifrequency tomography using P, PP and P-diffracted waves. *Geophysical Journal International*, v. 220 (1), pp.96-141.
- Housen, B.A. and Dorsey, R.J., 2005, Paleomagnetism and tectonic significance of Albian and Cenomanian turbidites, Ochoco basin, Mitchell Inlier, central Oregon. *Journal of Geophysical Research: Solid Earth*, p. 1-22, 110(B7), doi:10.1029/2004JB003458.
- Humphreys, E.D., Schmandt, B., Bezada, M.J., and Perry-Houts, J., 2015, Recent craton growth by slab stacking beneath Wyoming: *Earth and Planetary Science Letters*, v. 429, p. 170–180, doi: 10.1016/j.epsl.2015.07.066 .Müller, R.D., Sdrolias, M., Gaina, C., and Roest, W.R., 2008, Age, spreading rates, and spreading asymmetry of the world's ocean crust: *Geochemistry, Geophysics, Geosystems* – G3, v. 9, doi: 10.1029/2007GC001743.
- Humphreys, E., 2009, Relation of flat subduction to magmatism and deformation in the western United States, in Kay, S.M., Ramos, V.A., and Dickinson, W.R., eds., *Backbone of the Americas: Shallow Subduction, Plateau Uplift, and Ridge and Terrane Collision: Geological Society of America Memoir* 204, p. 85-98, doi: 10.1130/2009.1204(04)
- Irving, E., 1985, Whence British Columbia: *Nature*, v. 314, p. 673-674.
- Jicha, B.R. and Kay, S.M., 2018, Quantifying arc migration and the role of forearc subduction erosion in the central Aleutians. *Journal of Volcanology and Geothermal Research*, 360, p. 84-99.

- Johnston, S.T., 2008, The Cordilleran ribbon continent of North America: *Annual Review of Earth and Planetary Sciences*, v. 36, p. 495–530, doi: 10.1146/annurev.earth.36.031207.124331.
- Johnston, S.T., 2001, The Great Alaskan Terrane Wreck: reconciliation of paleomagnetic and geological data in the northern Cordillera: *Earth and Planetary Science Letters*, v. 193, p. 259–272.
- Kent, D.V., and Irving, E., 2010, Influence of inclination error in sedimentary rocks on the Triassic and Jurassic apparent pole wander path for North America and implications for Cordilleran tectonics: *Journal of Geophysical Research B, Solid Earth*, v. 115, p. 1-25, doi: 10.1029/2009JB007205.
- Leonard, L.J., Hyndman, R.D., Mazzotti, S., Nykolaishen, L., Schmidt, M. and Hippchen, S., 2007, Current deformation in the northern Canadian Cordillera inferred from GPS measurements. *Journal of Geophysical Research: Solid Earth*, v. 112, p. 1-15, B11401, doi:10.1029/2007JB005061
- Livaccari, R. F., Burke, K. & Sengor, A. M. C., 1981, Was the Laramide orogeny related to subduction of an oceanic plateau? *Nature* v. 289, p. 276–278.
- Mihalynuk, M.G. and Diakow, L.J., 2020, Southern Nicola arc geology. British Columbia Ministry of Energy, Mines and Low Carbon Innovation, British Columbia Geological Survey Geoscience Map 2020-01, 1:50,000 scale, two sheets.
- Mihalynuk, M.G., Erdmer, P., Ghent, E.D., Cordey, F., Archibald, D.A., Friedman, R.M., and Johannson, G.G., 2004, Coherent French Range blueschist: Subduction to exhumation in < 2.5 m.y.?: *Geological Society of America Bulletin*, v. 116, p. 910–922, doi: 10.1130/b25393.
- Monger, J.W. and Gibson, H.D., 2019, Mesozoic-Cenozoic deformation in the Canadian Cordillera: The record of a “Continental bulldozer”?. *Tectonophysics*, v. 757, p.153-169.
- Moore, E.M., 1970, Ultramafics and orogeny, with models of the US Cordillera and the Tethys: *Nature*, v. 228, p. 837–842.
- Moore, E.M., 1998, Ophiolites, the Sierra Nevada, “Cordillera,” and orogeny along the Pacific and Caribbean margins of North and South America: *International Geology Review*, v. 40, p. 40–54.
- Morgan, W.J., 1983, Hotspot tracks and the early rifting of the Atlantic. In *Developments in geotectonics* (Vol. 19, pp. 123-139). Elsevier.
- Müller, R.D., Sdrolias, M., Gaina, C., and Roest, W.R., 2008, Age, spreading rates, and spreading asymmetry of the world’s ocean crust: *Geochemistry, Geophysics, Geosystems – G3*, v. 9, doi: 10.1029/2007GC001743.
- O’Neill, C., Mueller, D., and Steinberger, B., 2005, On the uncertainties in hot spot reconstructions and the significance of moving hot spot reference frames: *Geochemistry, Geophysics, Geosystems – G3*, v. 6, doi: 10.1029/2004GC000784.
- Paterson, S.R. and Ducea, M.N., 2015, Arc magmatic tempos: Gathering the evidence. *Elements*, 11(2), p. 91-98.
- Patton Jr, W.W. and Box, S.E., 1989, Tectonic setting of the Yukon-Koyukuk basin and its borderlands, western Alaska. *Journal of Geophysical Research: Solid Earth*, 94(B11), p. 15807-15820.8, DOI: 10.2113/gselements.11.2.91
- Pavlis, G.L., Sigloch, K., Burdick, S., Fouch, M.J., and Vernon, F.L., 2012, Unraveling the geometry of the Farallon plate: Synthesis of three-dimensional imaging results from USArray: *Tectonophysics*, v. 532–535, p. 82–102, doi: 10.1016/j.tecto.2012.02.008.

- Pavlis, T.L., Amato, J.M., Trop, J.M., Ridgway, K.D., Roeske, S.M. and Gehrels, G.E., 2019, Subduction polarity in ancient arcs: A call to integrate geology and geophysics to decipher the Mesozoic tectonic history of the Northern Cordillera of North America. *GSA Today*, 29(11), pp.4-10.
- Ribe, N.M., Stutzmann, E., Ren, Y., and van der Hilst, R., 2007, Buckling instabilities of subducted lithosphere beneath the transition zone: *Earth and Planetary Science Letters*, v. 254, p. 173–179, doi: 10.1016/j.epsl.2006.11.028.
- Saleeby, J., and Dunne, G., 2015, Temporal and tectonic relations of early Mesozoic arc magmatism, southern Sierra Nevada, California, in Anderson, T.H., Didenko, A.N., Johnson, C.L., Khanchuk, A.I., and MacDonald, J.H., Jr., eds., *Late Jurassic Margin of Laurasia—A Record of Faulting Accommodating Plate Rotation: Geological Society of America Special Paper 513*, p. 223–268, doi:10.1130/2015.2513(05).
- Schweickert, R.A., 2015, Jurassic evolution of the Western Sierra Nevada metamorphic province, in Anderson, T.H., Didenko, A.N., Johnson, C.L., Khanchuk, A.I., and MacDonald, J.H., Jr., eds., *Late Jurassic Margin of Laurasia—A Record of Faulting Accommodating Plate Rotation: Geological Society of America Special Paper 513*, p. 299–358, doi:10.1130/2015.2513(08).
- Seton, M., Müller, R.D., Zahirovic, S., Gaina, C., Torsvik, T., Shephard, G., Talsma, A., Gurnis, M., Turner, M., Maus, S., and Chandler, M., 2012, Global continental and ocean basin reconstructions since 200 Ma: *Earth-Science Reviews*, v. 113, p. 212–270, doi: 10.1016/j.earscirev.2012.03.002.
- Sigloch, K., 2008, *Multiple-Frequency Body-Wave Tomography* [Ph.D. thesis]: Princeton, New Jersey, Princeton University, 249 p.
- Sigloch, K., 2011, Mantle provinces under North America from multifrequency P-wave tomography: *Geochemistry Geophysics Geosystems*, v. 12, Q02W08, doi: 10.1029 /2010GC003421 .
- Sigloch, K., and Mihalynuk, M.G., 2013, Intra-oceanic subduction shaped the assembly of Cordilleran North America: *Nature*, v. 496, p. 50–56, doi: 10 .1038/nature12019 .
- Sigloch, K. and Mihalynuk, M.G., 2020, Comment on GSA Today article by Pavlis et al., 2019:“Subduction polarity in ancient arcs: A call to integrate geology and geophysics to decipher the Mesozoic tectonic history of the northern Cordillera of North America”. *GSA Today*, v. 30, p. e47-e50, <https://doi.org/10.1130/GSATG431C.1>.
- Sigloch, K., McQuarrie, N., and Nolet, G., 2008, Two-stage subduction history under North America inferred from multiple-frequency tomography: *Nature Geoscience*, v. 1, p. 458–462, doi: 10 .1038 /ngeo231 .
- Tardy, M., Lopicier, H., Bourdier, J.L., Coulon, C., Hernández, L.E.O. and Yta, M., 1992, Intraoceanic setting of the western Mexico Guerrero terrane--implications for the Pacific-Tethys geodynamic relationships during the Cretaceous. *Revista mexicana de ciencias geológicas*, 10(2), pp.118-128.
- Tepper, J.H., and Clark, K.P., 2024, Initiation of the Cascade arc: *Geology*, v. 52, p. 297–301, <https://doi.org/10.1130/G51888.1>
- Tikoff, B., Housen, B.A., Maxson, J.A., Nelson, E.M., Trevino, S., and Shipley, T.F., 2023, Hit-and-run model for Cretaceous–Paleogene tectonism along the western margin of Laurentia, in Whitmeyer, S.J., Williams, M.L., Kellett, D.A., and Tikoff, B., eds., *Laurentia: Turning Points in the Evolution of a Continent: Geological Society of America Memoir 220*, p. 659–705, [https://doi.org/10.1130/2022.1220\(32\)](https://doi.org/10.1130/2022.1220(32)).
- Tomek, F., Žák, J., Verner, K., Ježek, J. and Paterson, S.R., 2024, A complex interplay between pluton emplacement, tectonic deformation, and plate kinematics in the Cretaceous Sierra Nevada magmatic arc, California. *Tectonics*, 43(3), p.e2023TC007822.

- Torsvik, T.H., Steinberger, B., Shephard, G.E., Doubrovine, P.V., Gaina, C., Domeier, M., Conrad, C.P. and Sager, W.W., 2019, Pacific-Panthalassic reconstructions: Overview, errata and the way forward. *Geochemistry, Geophysics, Geosystems*, 20(7), p. 3659-3689.
- Tosdal, R.M., and Wooden, J.L., 2015, Construction of the Jurassic magmatic arc, southeast California and southwest Arizona, in Anderson, T.H., Didenko, A.N., Johnson, C.L., Khanchuk, A.I., and MacDonald, J.H., Jr., eds., *Late Jurassic Margin of Laurasia—A Record of Faulting Accommodating Plate Rotation: Geological Society of America Special Paper 513*, p. 189–221, doi:10.1130/2015.2513(04).
- Van der Meer, D.G., Van Hinsbergen, D.J. and Spakman, W., 2018, Atlas of the underworld: Slab remnants in the mantle, their sinking history, and a new outlook on lower mantle viscosity. *Tectonophysics*, 723, p. 309-448.
- Wessel, P. and Kroenke, L.W., 2008, Pacific absolute plate motion since 145 Ma: An assessment of the fixed hot spot hypothesis. *Journal of Geophysical Research: Solid Earth*, 113(B6).
- Wright, J.E. and Wyld, S.J., 2007, Alternative tectonic model for Late Jurassic through Early Cretaceous evolution of the Great Valley Group, California.

Figure captions

Figure 1. Observations for tomotectonics: subducted lithosphere (slabs) in the mantle and a quantitative plate reconstruction at the surface. Coloured polygons show outlines of major slabs under North America from the regional tomographic P-wave model of Sigloch (2011). Orange slabs were deposited by westward subduction, green slabs by eastward (Farallon) subduction. Dark shades are applied to lower-mantle slabs MEZ, ANG and CR/W; light shades to (mostly) shallower slabs FS (400-1000 km deep), FN (0-700 km), and to the shallow western end of ANG (>400 km deep).

Superimposed are snapshots in time showing the westward migrating margin of North America in a mantle reference frame constrained between 0-120 Ma by moving hotspots (Dobrovine et al., 2012) and 120-170 Ma by true polar wander-corrected paleomagnetic data (Torsvik et al., 2019). Under the tomotectonic null hypothesis, a continental margin above a slab indicates a continent-trench interaction. In such cases, barbs are drawn on the continental margin in order to signal the nature of the interaction: NAM-beneath-arc collision (orange barbs, associated with westward subduction) or ocean plate beneath margin, with arc built on NAM (green barbs, associated with eastward subduction). A transform regime along the ocean-continent boundary is marked in light blue, with blue arrows for displacement direction. Transform motion can be inferred from the continent margin overlying a slab-free zone, but only if the margin is known to be a plate boundary (prior to ~150 Ma, it was not). Yellow line signals the western edge of FS slab, associated with the “Big Break” event of transition from subduction to transform ~80 Ma. During a short time window around ~70 Ma, the entire margin is inferred to have been in a transform regime. The starting point of our inference is ~170 Ma, the time when North America separated from Pangaea, and when absolute paleo-positioning in plate reconstructions becomes reasonably accurate.

Figure 2. Subducted oceanic lithosphere (slab) deposited in the mantle by past and present Farallon subduction at latitudes of the Pacific Northwest, from the surface to ~1800 km depth. Seismically fast structure (subducted oceanic lithosphere) is rendered as 3-D isosurfaces (threshold $dV_p/V_p > 0.25\%$) on the teleseismic P-wave model of Sigloch 2011. Color signals depth and changes in increments of 200 km. Surface topography of the North American Cordillera and the Pacific basin are overlain in translucent

gray, with strong vertical exaggeration. Yellowstone (red triangle) and its vertical downward continuation are shown for visual reference. Not rendered are seismically slow anomalies (such as the Yellowstone mantle plume, which is wedged inside the “cavities” of the slabscape).

The slab has an overall eastward dip. In detail, its geometries are complex and fragmented, but highly structured. The slab is clearly delineated against adjacent and deeper slab-free areas. It enters the mantle with the thickness of lithosphere (<100 km, purple parts), but thickens in the transition zone (blues) and is most massive in the lower mantle (green, yellow, red). The shallow fast anomalies of the Wyoming craton and lithosphere of stable NAM had to be masked out as they are located between the viewpoint of the figure and the slabscape.

Figure 3. Mantle tomography: 3-D isosurface rendering of all seismically fast P-wave anomalies in the upper and lower mantle beneath North America to ~1800 km depth. The rendering threshold is $dV_p/V_p = +0.25\%$. Below lithospheric depths, fast anomalies can generally be taken to mean slab (subducted lithosphere). (A) top-down view of all fast structure below 400 km (in order to exclude the overlying lithosphere, which is fast but not slab). Color signals depth and changes every 200 km. (B) inside-out view of all fast structure from the surface down, with the deepest structure (slab walls) emerging to the foreground. Imaging limitations include artifacts, especially near the margins of the regional dataset: resolution lost into the ocean basins and north of 55° . Two downward smearing artifacts are labeled with white x's and should not be interpreted. (After Sigloch, 2011.)

Figure 4. Illustration of the tomotectonic null hypothesis. Range of possible shapes for slabs that sink *vertically* after entering the trench (and grow long enough to enter the lower mantle). Dashed line represents the viscosity discontinuity between upper mantle (UM) and lower mantle (LM), where the mantle becomes 1-2 orders of magnitude more viscous, resisting further slab sinking. This cartoon explores the parameter space of relevant ratios of the three velocities that determine slab geometry: (1) convergence velocity onto the trench of the subducting plate (v_{sp}); (2) trench retreat velocity of the overriding plate (v_t); (3) velocity at which the slab tip in the LM can sink vertically $v^{z_{tip}}$. Vectorial arrows for v_t , v_{sp} , $v^{z_{tip}}$ are shown qualitatively for each slab cartoon; $v^{z_{tip}}$ is arbitrarily chosen as constant across the different cases.

Trench retreat velocity v_t (normalized by $v^{z_{tip}}$) is shown on the x-axis. If the trench is stationary ($v_t = 0$), a vertical slab piles up beneath it. Trench retreat ($v_t > 0$) produces a trenchward dipping slab: the dip results from recently subducted slab not yet having sunk as far as older slab. Trench advance ($v_t < 0$, rarely observed) produces an overturned dipping slab. Kinematic ratio K_r on the y-axis expresses whether v_{sp} , the length of slab newly entering the mantle per time unit, can be accommodated in the slab-free space created by trench migration v_t (horizontally away from already-deposited slab) and/or by the vertical sinking away of older slab ($v^{z_{tip}}$), which vacates upper-mantle space. $K_r > 1$ indicates “traffic jam conditions”, where plate convergence is too rapid to be accommodated undeformed, so the slab is forced to thicken (probably by folding). Tomography observes thickened slabs to be ubiquitous in the lower mantle. Consistent with this, Cerpa et al. (2022) found that $K_r > 1$ for almost all present-day trenches. See Cerpa et al. (2022) for exact definition of K_r .

Figure 5. Paleo-trenches in absolute (mantle) coordinates, as predicted by tomotectonics and its vertical slab sinking hypothesis. This represents a quasi-literal transcription of the 3-D slabscape with depth. Tracks of paleo-arc locations are shown as thick lines if produced by westward subduction, and thin lines if produced by eastward subduction or subduction of ambiguous polarity (mostly Farallon). For laterally

extended slabs, those produced when the arc translates rapidly with respect to the mantle reference frame, a distinct locus of slab deposition is not clearly resolvable, and the arc lines are shown as dashed. Depth-to-colour mapping as for the slab-scapes of figures 2 & 3. The colour bar also shows an indicative depth-to-time mapping. This time conversion is empirically justified by the observation that slabs seem to have sunk rather uniformly at a rate of ~ 10 mm/yr. This averaged sinking rate is a parameter estimated from slab geometries and plate motions; a constant sinking rate is *not* assumed, neither is it part of the tomotectonic hypothesis. It is not strictly needed for this study, but remains useful as a rough and robust link to geologic time. The continent is reconstructed at three times 170 Ma, ~ 80 Ma (green outline), and present day. Grey tones denote 2D extents of slabs of concern at 800 km depth (light grey) and 1400 km (medium grey). Arc / slab labels: A = Aleutian, ANG = Angayucham, KI = Kula-Izanagi, MEZ = Mezcalera. SN = approximate position of the Sierra Nevada batholith; the arrow denotes possible extents of the Hess-Shatsky Rise conjugate plateau.

Figure 6. Constraints on the growth and consumption of ocean basins subducting into the Archipelago, shown in two cartoon time frames for 170 Ma (early Archipelago before NAM started moving west) and for 80 Ma (override far advanced, westward subduction almost overridden). Trenches highlighted with barbs and colours were active at 170 Ma (red) or 80 Ma (green); they are plotted on the basemap of fig. 4. The lateral distance from continent (or Farallon spreading ridge) to its nearest slab defines the extents of two paleo-oceans: the Farallon Ocean subducted eastward, the Mezcalera-Angayucham Ocean (NAM plate) westward. Lateral overlap of continent and trench predicts a continent-arc collision. Trenches at 170 Ma run above the three slab walls that all reach to ~ 1800 - 2000 km depth – representing the early, purely intra-oceanic stage of the archipelago. Farallon and ANG subduction face each other off in double-sided subduction from the start. The width of CR slab corresponds to the (narrow) width of early Farallon isochrons (FAR-PAC-Izanagi spreading “triangle” at 170 Ma). Baja-BC shuffling and assembly of Alaska will play in the small space between these two arcs, on the Orcas microplate. The mature Pacific-Farallon spreading ridge at 80 Ma “serves” both CR and FS, where FS is a margin-hugging trench, whereas CR (the original, northern Farallon) still remains offshore.

Figure 7. Arc terranes matched to slabs. Arc (super-)terranes are shown in their present positions in the Cordillera on the left part of the map. The same arc terranes are schematically reconstructed above their matched slabs and paleo-trenches, in absolute positions relative to the lower mantle. The reconstruction time for the arcs and slab walls corresponds to ~ 170 Ma (before Archipelago override began), except in the case of the SW-ward migrating southern Farallon (SNB) arc, which is shown in several time snapshots migrating across the area it covered over its lifetime (~ 130 - 80 Ma). Current and former instances of arcs are linked by their unchanging colors over time: Farallon arcs and slabs in green, Insular (INS) & Guerrero (GUE) microcontinents and slabs in orange; Intermontane (IMS) microcontinent in purple; and Central Alaskan arcs and slabs in red. Westward drift of North America is shown at 170 Ma, 140 Ma and 80 Ma (green coastline), as calibrated from Atlantic ocean isochrons and a mantle reference frame. Every substantive slab should be associated with a geologically known arc, and every known arc should be associated with a slab. The above slab/terranes associations appear to satisfy geologic constraints, and to yield the Cordillera’s present-day terrane assemblage when the 150 million years of slab-predicted collision sequences are played forward.

Abbreviations: Guerrero-Insular arc terranes (orange) include basement substrate, with arcs constructed atop by westward subduction: AX (Alexander), GU (Guerrero), PE (Peninsular), WF (Western Jurassic, Western Hayfork, Foothills, and related terranes), WR (Wrangellia), SA (Santa Ana). IMS Superterrane (purple) include terranes docked at the margin of North America before or immediately following the start of Atlantic spreading: BM (Blue Mountains), CC (Cache Creek), QN (Quesnel), ST (Stikine) and YTT

(Yukon Tanana). Terranes linked to the Native Jurassic arc (NJ) and its along-strike continuation of extensional magmatism in Mexico (“Nazas arc”) are diagrammatically shown by purple asterisks. Green terranes are associated with Farallon subduction (eastward): CG—Chugach; FR—Franciscan; PR—Pacific Rim; SC—Siletz-Crescent; VC—Vizcaino. Cyan polygons are suture basins – the relics of large paleo-ocean basins shown in translucent cyan; they straddle the boundary between orange (MEZ) and purple (IMS/NJ) terranes as predicted. Where adjacent IMS was below sea level, the suture basin strata may have extended as the Bowser Basin (BB). Sierra Nevada batholith, located immediately east of basin 10, overprints the basin and the Native Jurassic arc. (Modified from Sigloch & Mihalynuk, 2017.)

Figure 8. Collisional deformation since ~155 Ma, when NAM first rode into the archipelago, welded into its westward-subducting plate. Progression of deformation is shown (A) in three time slices of cartoon cross sections through crust and mantle, and (B) in the eastward progression of dated faults (triangles) and folds (diamonds) in the western USA and southwest Canada. (A) At 160 Ma, arc magmatism above the westward-subducting Mezcalera Ocean, at the leading edge of North America (NAM), adds crust to the Insular Superterrane (INS) arc and lithosphere to the MEZ slab wall. Circa 155 Ma, the last of Mezcalera lithosphere is consumed between NAM and easternmost INS: NAM collides with INS microcontinent, resulting in Nevadan deformation at the California margin and upward truncation of the slab wall (140 Ma panel). Further manifestations of this continent-microcontinent collision are deformation in the Omenica Belt of southern Canada, and deposition of the first west-derived sediments in the Western Canadian Sedimentary Basin, the Late Jurassic Passage Beds. As NAM is still being pulled westward (by intact trench segments in and out of the figure plane), subduction polarity at the collided segment is forced to flip, resulting in a new margin-hugging arc, including the Sierra Nevada batholith (SNB), which overprints the NAM-INS suture. Slab deposited by eastward (southern Farallon) subduction creates an east-dipping blanket (100 Ma panel) as the trench is forced westward in front of advancing NAM. Both north and south of the initial collision site, NAM continues to collide with microcontinental INS, resulting in widening Sevier deformation (Columbian orogeny in Canada), which is driven continually eastward. Map (B) shows this eastward and outward progression of deformation with dated faults and folds, using the same color-time conversion as trenches in (A), 20 m.y. per color increment.

Figure 9. Margin-parallel terrane translations based principally on paleomagnetic data from Late Cretaceous and Eocene strata. These data constrain the tomotectonic terrane reconstruction model of Clennett et al. (2020), which is modified in the figures. (A) Present-day terrane map shows the current locations of a half-dozen units that are very robustly constrained. The green/blue lines (with dates in Ma at nodes) represent spatio-temporal trajectories into the past of these units, back to where they were deposited, according to our Clennett et al. 2020 reconstruction. This reconstruction honors the constraints of the most solid paleomag sites, Carmacks & Mount Tatlow/Churn Creek, but Spences Bridge paleomag is not honored since it does not fully pass the fold test. Magnitudes of terrane offsets in the model are consistent with the paleomagnetic data. Trajectories are modeled in absolute coordinates relative to the lower mantle. The *main* BajaBC translations are implemented 70-50 Ma along the yellow line, which runs mainly through Intermontane terranes (and their left-behind correlatives in the Blue Mountains/U.S.). This Baja-BC fault line is necessarily speculative, but it must run inboard of all paleomag sites that show significant offsets (details in section 6.2). Accreted superterrane packages are colored as in fig. 7; additional pericratonic blocks are colored dark and light purple.

(B) 85 Ma snapshot reconstructing the assembly of Alaska. Tomotectonically inferred the northward sprint of Baja-BC, and its accretion to the arcs of future Central Alaska. These events occur on the Orcas

microplate (MP), the space between the two old, stationary ANG (red barbs) and Farallon CR trenches (green barbs). The future Central Alaskan arcs (red) are gradually dislodged from their SW-ward subducting ANG slab as NAM overrides obliquely – the “Great Alaskan Terrane Wreck” of Johnston (2001). BajaBC (INS and western IMS in Canada) has arrived from the south along the yellow main shear fault and are now quasi part of the Orcas MP, separated from the NAM plate by the main fault (yellow line). Baja-BC passes *inboard* of, and unimpeded by, the CR Farallon trench, which still sits offshore. The Orcas MP is small and displaceable; as NAM pushes westward, Orcas is squeezed out toward the west or northwest, probably subducting into the area of the gray oval (a small upper mantle-slab overlying the CR slab, see text). Due to the small size of the plate, its disappearance can be very rapid, and the Baja-BC and Central Alaskan terranes follow along. As the Orcas seafloor subducts, the Farallon trench persists and makes landfall on NAM. Baja-BC and Central Alaska collapse against each other and against NAM, completing the assembly of Alaska. The angle between the yellow line (paralleling the NAM margin) and the ANG slab (red line) sets the angle of the future Alaskan orocline. Override and SW-ward subduction finishes ~55 Ma according to slab geometries. The offshore CR trench converts into the margin-hugging Cascades trench, closing off this northwestern passage for shuffling terranes.